HHS Public Access

Author manuscript

Dev Biol. Author manuscript; available in PMC 2016 December 01.

Published in final edited form as:

Dev Biol. 2015 December 1; 408(1): 41–55. doi:10.1016/j.ydbio.2015.10.005.

The Endocytic Recycling Regulatory Protein EHD1 Is Required for Ocular Lens Development

Priyanka Arya[1,2], **Mark A. Rainey**[2], **Sohinee Bhattacharyya**[2,3], **Bhopal Mohapatra**[2,4], **Manju George**[2], **Murali R Kuracha**[5], **Matthew D. Storck**[2], **Vimla Band**[1,2,6], **Venkatesh Govindarajan**[5,*], and **Hamid Band**[1,2,3,4,6,*]

[1]Department of Genetics, Cell Biology & Anatomy, College of Medicine, University of Nebraska Medical Center, 985805 Nebraska Medical Center Omaha, NE, 68198-5805, USA

[2]Eppley Institute for Research in Cancer and Allied Diseases, University of Nebraska Medical Center, 985950 Nebraska Medical Center, NE, 68198-5950, USA

[3]Department of Pathology & Microbiology, College of Medicine, University of Nebraska Medical Center, 985900 Nebraska Medical Center Omaha, NE, 68198-5900, USA

[4]Department of Biochemistry & Molecular Biology, College of Medicine, University of Nebraska Medical Center, 985870 Nebraska Medical Center Omaha, NE, 68198-5870, USA

[5]Department of Biomedical Sciences, Creighton University, 2500 California Plaza, Omaha, NE, 68178, USA

[6]Fred & Pamela Buffett Cancer Center, University of Nebraska Medical Center, 985950 Nebraska Medical Center Omaha, NE, 68198-5950, USA

Abstract

The C-terminal Eps15 homology domain-containing (EHD) proteins play a key role in endocytic recycling, a fundamental cellular process that ensures the return of endocytosed membrane components and receptors back to the cell surface. To define the *in vivo* biological functions of EHD1, we have generated *Ehd1* knockout mice and previously reported a requirement of EHD1 for spermatogenesis. Here, we show that approximately 56% of the *Ehd1-null* mice displayed gross ocular abnormalities, including anophthalmia, aphakia, microphthalmia and congenital cataracts. Histological characterization of ocular abnormalities showed pleiotropic defects that include a smaller or absent lens, persistence of lens stalk and hyaloid vasculature, and deformed optic cups. To test whether these profound ocular defects resulted from the loss of EHD1 in the lens or in non-lenticular tissues, we deleted the *Ehd1* gene selectively in the presumptive lens ectoderm using *Le-Cre*. Conditional *Ehd1* deletion in the lens resulted in developmental defects that included thin epithelial layers, small lenses and absence of corneal endothelium. *Ehd1*

[*]Corresponding authors: 1. Hamid Band, MD, PhD, University of Nebraska Medical Center, Omaha, Nebraska, 68198-5950, USA; Tel: 402-559-8572 (Office), Fax: 402-559-4651, hband@unmc.edu, 2. Venkatesh Govindarajan, PhD. Department of Biomedical Sciences, Creighton University, 2500 California Plaza, Omaha, NE, 68178, USA; Tel: 402-280-1819 (Office), Fax: 402-280-2690, g.v@creighton.edu.

deletion in the lens also resulted in reduced lens epithelial proliferation, survival and expression of junctional proteins E-cadherin and ZO-1. Finally, *Le-Cre*-mediated deletion of *Ehd1* in the lens led to defects in corneal endothelial differentiation. Taken together, these data reveal a unique role for EHD1 in early lens development and suggest a previously unknown link between the endocytic recycling pathway and regulation of key developmental processes including proliferation, differentiation and morphogenesis.

Keywords

Endocytic recycling; EHD1; lens development; apoptosis; proliferation; polarity; lens epithelium; corneal endothelium

Introduction

Endocytic traffic represents a fundamental cellular process conserved in most eukaryotes (Maxfield and McGraw, 2004). Cell biological studies have demonstrated that cell surface receptors as well as membrane lipids are constantly internalized at rates determined by cellular activities such as uptake of nutrients, stimulation by extracellular ligands as well as uptake of particulate materials (B. D. Grant and Donaldson, 2009). Internalized receptors may be targeted for degradation in the lysosomes, often depending on the stimulating ligands, or recycled back to the cell surface together with membrane lipid components. The process of endocytic recycling is also used adaptively to orchestrate trans-cellular transport processes and selective localization of surface lipids and receptors to specific membrane domains in polarized cells (Scita and Di Fiore, 2010). The recycling pathway also appears to play an important role in a variety of other cell biological processes such as membrane repair, cytokinesis (Montagnac et al., 2008), cell migration (Jones et al., 2006) and developmental patterning (Bokel and Brand, 2014).

C-terminal Eps15 homology domain-containing (EHD) proteins are a recently described family of endocytic recycling regulatory proteins (B. D. Grant and Caplan, 2008). The role of EHD proteins in endocytic traffic was first revealed through identification of *rme-1* (*receptor-mediated endocytosis 1*) mutant in *C. elegans*, which impaired the yolk protein transport across the intestinal epithelium into coelom (Lin et al., 2001). Cell biological studies demonstrated that RME-1 as well as a human ortholog EHD1 localized to an endocytic recycling compartment and EHD function was required for transferrin recycling and retrograde transport of a reporter protein to the trans-Golgi network (George et al., 2007; B. Grant et al., 2001; Lin et al., 2001). Mammals express four highly homologous EHD proteins (EHD1–4). EHD1 has been most extensively studied in cellular models and shown to be required for endocytic recycling of a number of other cell surface receptors, including transferrin receptor (Lin et al., 2001), MHC-I (Caplan et al., 2002), MHC-II molecules (Walseng et al., 2008), β1-integrin (Scheiblin et al., 2014) and GLUT4 glucose transporter (Guilherme et al., 2004).

All four EHD proteins contain an N-terminal ATPase/GTPase domain that controls membrane binding and oligomerization, a central coiled-coiled domain that mediates homo- and hetero-oligomerization, and a characteristic C-terminal EH domain that mediates

interactions with proteins containing Asn-Pro-Phe (NPF) or related tri-peptide motifs (de Beer et al., 2000; B. D. Grant and Caplan, 2008; Kieken et al., 2007; Kieken et al., 2010). Biochemically, EHD proteins are thought to facilitate membrane tubulation and scission to facilitate vesicle budding and transport in the recycling pathway (Daumke et al., 2007). Crystal structure of EHD2 revealed it to be a dimer and it is presumed that other family members adopt a similar conformation (Daumke et al., 2007). EHD proteins form homo- or hetero-dimers, thought to facilitate EHD function (Daumke et al., 2007; Lee et al., 2005; Naslavsky and Caplan, 2011). Consistent with their structural relatedness, reconstitution of rme-1 mutant worms with each of the four human EHD proteins led to restoration of function (George et al., 2007).

In vitro studies have suggested that EHD3 and EHD4 mediate early steps of membrane-associated receptor recycling whereas EHD1 and EHD2 regulate later steps (George et al., 2007; Sharma et al., 2008). Several lines of evidence point to unique functional roles of individual EHD proteins, despite their structural similarities. EHD protein expression in mammalian tissues shows discrete patterns and distinct family members predominate within different cell types within complex tissues. Loss of one family member can trigger compensatory increase of another, but this too appears to differ with cell/tissue compartments (George et al., 2011; Rainey et al., 2010). Biochemical studies also indicate that individual EHD proteins may preferentially dimerize with distinct family members (Lee et al., 2005). Thus, it is likely that individual EHD proteins serve distinct physiological roles despite their shared biochemical mechanisms.

In order to define the biological roles of mammalian EHD family proteins, we and others have generated mouse gene deletion models. These models reveal unique as well as redundant roles of EHD proteins in vivo. *EHD1* deletion exhibits a strain-dependent phenotype. *Ehd1* mutant mice on 129Sv/Ev or Swiss Webster background appeared normal (Rapaport et al., 2006). In contrast, *Ehd1-null* mice on a mixed 129/B6 background exhibit pre-natal lethality, reduced size and male infertility (Rainey et al., 2010). Further studies indicated that *Ehd1-null* mice exhibit smaller muscle fibers, consistent with a role of EHD1 in myocytes proliferation and fusion (Posey et al., 2014).

Deletion of *Ehd3* or *Ehd4* has no apparent impact on prenatal mouse development but *Ehd4–null* male mice exhibited smaller testes and reduced fertility (George et al., 2010; George et al., 2011). Further studies of *Ehd3-null* mice have revealed cardiac abnormalities including arrhythmias and blunted response to adrenergic stimulation together, with reduced expression of Na/Ca exchanger (NCX1), L-type Ca-channel type 1.2 ($Ca_v1.2$) and associated functions (Curran et al., 2014; Gudmundsson et al., 2010). Notably, mice with combined *Ehd3* and *Ehd4* resulted in high pre- and peri-natal mortality, with surviving animals exhibiting severe renal thrombotic microangiopathy and death due to renal failure (George et al., 2011). These initial studies support the approach of using knockout models to define specific as well as redundant biological roles of the EHD family of endocytic regulators.

Previously, we noted that *Ehd1-null* mice on 129/B6 background exhibited ocular abnormalities, but these were not characterized in any detail (Rainey et al., 2010). Here, we

provide evidence that EHD1 is required for the development of ocular lens and cornea. Our studies show that *Ehd1-null* mice display pleiotropic ocular phenotypes, including anophthalmia, aphakia, microphthalmia and congenital cataracts. Importantly, conditional deletion of *Ehd1* in the presumptive lens ectodermal cells recapitulated the lenticular phenotypes observed in *Ehd1-null* mice, and also resulted in corneal endothelial differentiation defects. The ocular phenotypes caused by the loss of a single regulator of endocytic recycling, *Ehd1*, provides a novel model system to elucidate mechanistic links between surface receptor recycling and control of cellular processes that ensure orderly development of the compartments of mammalian eye.

Materials and Methods

Mouse models and genotyping

Ehd1$^{flox/flox}$ mice, harboring a conditionally-targeted *Ehd1* allele in which exon 1 is flanked by loxP sites, and whole-body knockout mice (*Ehd1-null*) derived from *Ehd1*$^{flox/flox}$ mice have been described previously (Rainey et al., 2010). *Ehd1-null* mice were maintained on mixed 129;B6 background. Single nucleotide polymorphism (SNP) analysis (DartMouse, Lebanon, NH) revealed these to have ∼70% contribution from the C57Bl/6 genome (supplementary Fig. S1). *Ehd1-WT* (wild type), *Ehd1-het* (heterozygous), and *Ehd1-null* (homozygous null) mice were generated by mating *Ehd1-het* mice. Breeders were maintained on high-fat chow (# 2019, Harlan Laboratories Inc., Madison, WI). Genomic DNA was extracted from embryonic yolk sacs or adult tail tips with proteinase K digestion, isopropanol precipitation and used for genotyping as described previously (Rainey et al., 2010). To conditionally delete *Ehd1* in the lens, *Ehd1*$^{flox/flox}$ mice (backcrossed more than 6 generations into C57BL/6J, and 98% C57Bl/6 by DartMouse SNP typing) were crossed with *Le-Cre* transgenic mice (maintained in a hemizygous manner on an FVB/N background), which expresses Cre recombinase from a Pax6 promoter active in the lens-forming ectoderm by day E9.0 (Ashery-Padan et al., 2000a). This cross resulted in *Ehd1*$^{flox/+}$*;Le-Cre* mice. Subsequent back-cross to *Ehd1*$^{flox/flox}$ mice generated the *Ehd1*$^{flox/flox}$*;Le-Cre* genotype referred to as conditional knockout (CKO) mice. *Ehd1*$^{flox/flox}$ mice without the *Le-Cre* served as controls. To confirm *Le-Cre*-mediated deletion in the lens, genomic DNA samples were isolated from P0/P1 micro-dissected lenses from control and test pups and subjected to PCR analysis (data not shown) using *Ehd1*-specific primer pairs as described previously (Rainey et al., 2010). Embryos/mice were genotyped for the presence of *Le-Cre* transgene using the primer set 5'-GCATTACCGGTCGATGCAACGAGTGATGAG-3' and 5'-GAGTGAACGAACCTGGTCGAAATCAGTGCG-3'. All animal studies were approved by the Institutional Animal Care and Use Committee (# 07–061-FC12). Animals were treated humanely in accordance with the University of Nebraska Medical Center and the National Institute of Health (NIH) guidelines for the Care and the Use of Laboratory Animals.

Histology and Immunohistochemistry

For timed-pregnancy experiments, matings were set up in the evenings, and vaginal plugs were detected the following morning. The noon of the day of vaginal plug detection was considered E0.5. Pregnant dams were euthanized by CO_2 asphyxiation at the indicated time points and embryos were removed by hysterectomy. Embryonic yolk sacs were collected

and used for genotyping, as described above. Embryos were fixed at 4°C in 10% neutral-buffered formalin (NBF) for 3 to 12 hours, transferred to 70% ethanol prior to paraffin embedding and sectioned at 4–6 μm. Sections were stained with hematoxylin and eosin (H&E), and micrographs were captured using a Leica microscope or with an iScan Coreo Slide Scanner of the iScan Image Viewer (Roche) (at a resolution of 0.2325 micron per pixel) at the UNMC Tissue Sciences Facility. The total lens epithelial cell count was determined by counting hematoxylin-stained nuclei from serial sections of WT or *Ehd1 CKO* embryonic lenses using ImageJ software. Briefly, a line was drawn on 40x sagittal sections to demarcate the equatorial region where epithelial cells began to elongate and epithelial cells within this region were counted.

The following mouse monoclonal antibodies were used in immunofluorescence (IF) staining: anti-γ-Tubulin Clone GTU-88 (T5326; Sigma-Aldrich Corp, St. Louis, MO), anti-ZO-1 (1A12) (339100; Invitrogen, Camarillo, CA), anti-Bromodeoxyuridine (BrdU) Clone Bu20a (M0744; Dako, Carpinteria, CA), anti-a-Catenin (610193), anti-N-Cadherin (610920), anti-β-Catenin (610153) and anti-E-cadherin (610181) (all from BD-Transduction laboratories, Franklin Lakes, NJ). Rabbit polyclonal/monoclonal antibodies used were: anti-GFP (2555, Cell Signaling Technology, Beverly, MA), anti-Pax6 (PRB-278P; Covance, Princeton, NJ), anti-Pax-2 (71–6000; Invitrogen, Camarillo, CA), anti-keratin 12 (KAL-KR074, TransGenic Inc; Japan); anti- Prox1 (AB5475) and anti-Sox2 (AB5603) (from Millipore Corp., Massachusetts, MA); anti-γ-crystallin (a gift from Dr. Samuel Zigler, The Johns Hopkins University, School of Medicine, Baltimore, MD)(Russell et al., 1984); anti-alpha A Crystallin (ab5595) (Abcam Inc., Cambridge, MA); anti-β-crystallin (FL-252) (sc-22745; Santa Cruz Biotechnology, Dallas, Texas). Affinity-purified rabbit polyclonal anti-EHD1, rabbit anti-EHD2, anti-EHD3 and anti-EHD4 antisera were generated as described previously (George et al., 2007; George et al., 2010; George et al., 2011; Gudmundsson et al., 2010; Mate et al., 2012; Rainey et al., 2010; Sengupta et al., 2009).

For antibody staining, rehydrated tissue sections were boiled in antigen unmasking solution (H-3300, Vector Laboratories, Burlingame, CA) in a microwave for 20 min, slides were cooled, washed once in PBS, and blocked in heat-inactivated 10% Fetal Bovine Serum (SH30910.03, HyClone Laboratories, Logan, UT) for one hour at room temperature (RT). Primary antibodies diluted in blocking buffer were added overnight at 4°C (except EHD antibody staining, which was done at RT for an hour), slides were washed 3 times with PBS followed by incubation with Alexa Fluor 488 or 594-conjugated donkey anti-rabbit or anti-mouse secondary antibodies (1:200; Invitrogen, Carlsbad, CA) for one hour at RT in the dark. For negative controls, sections were incubated in the blocking buffer without the primary antibody. Nuclei were visualized with DAPI in antifade mounting medium (ProLong® Gold Antifade mountant, Invitrogen, Carlsbad, CA). Fluorescent images were captured on a Zeiss LSM-710 confocal microscope. Tiled images under 20x and 40x objectives were captured for embryonic eyes with 10% overlap and processed using the Zeiss Zen 2010 stitching software to merge into a single image. Z-stack images were captured under 63x objective at an optical slice of 0.56 μm. Images were processed using Adobe Photoshop CC software. For presentation, signal intensities were adjusted equally for brightness and contrast between control and test images.

BrdU and TUNEL labeling

Pregnant dams were injected intraperitoneally with 150 mg/kg of body weight of 10 mg/ml BrdU (5-bromo-2'-deoxyuridine) (Sigma-Aldrich, St. Louis, MO) and 1 mg/ml 5FU (5-fluoro-5'-deoxyuridine) (Sigma-Aldrich, St. Louis, MO) and sacrificed an hour later. Staining was performed on paraffin-embedded serial sections of embryo eyes using mouse anti-BrdU antibody. Images were captured with MagnaFire imaging software using Nikon Eclipse E600 Fluorescent microscope fitted with an Optronics camera. Cell proliferation was quantified by calculating the percentage of nuclei that were BrdU positive in a given section.

Terminal deoxynucleotidyl transferase (TdT)-mediated deoxyuridine triphosphate nick end labeling (TUNEL) assay, was performed on deparaffinized sections according to the manufacturer's instructions (Roche, Indianapolis, IN). Label solution without TdT was used as a negative control. Sections treated with DNase I (3 U/ml), to induce DNA strand breaks, served as positive controls. Slides were mounted with ProLong® mounting medium. TUNEL-positive cells were detected and quantified as with BrdU staining.

Statistical analysis

Serial sections from a minimum of four different embryos from at least three litters per time point were analyzed (N, number of embryos). Unpaired Student's t-test was used to analyze the significance of differences between experimental groups. Data are presented as mean ± standard error of the mean with $P \leq 0.05$ deemed significant.

Results

Ehd1-null mice exhibit ocular abnormalities

As described previously (Rainey et al., 2010), *Ehd1-null* mice on a mixed 129/B6 background are born at sub-Mendelian ratios and males were infertile due to defects in spermatogenesis. Close examination of adult *Ehd1-null* mice revealed a range of ocular defects, including microphthalmia, congenital cataracts, and anophthalmia (Fig. 1A, panels b–d) that were not seen in wildtype control mice (Fig. 1A, panel a). Approximately 56% of individual eyes in adult (6 weeks or older) *Ehd1-nullmice* displayed these defects, with cataracts being the most common defect (Table 1). To assess whether ocular defects were present in *Ehd1-null* mice during embryonic ocular development, WT and *EHD1-null* embryos were collected between embryonic (E) days E10.5-E18.5 and eye and lens morphologies were analyzed. Visual examination of whole embryos at E14.5 revealed pleiotropic ocular defects in *Ehd1-null* embryos (Fig. 1A, panels f–h, arrowheads), similar to those seen in adult mice, but not in wildtype controls (Fig 1A, panel e, arrow). Hematoxylin and eosin (H&E) staining of sections of embryonic ocular tissues revealed defects in *Ehd1-null* embryos as early as E10.5. At this age, the lens pit appeared smaller and misshapen (Fig. 1B, panels b & c, arrowheads) compared to wildtype controls (Fig. 1B, panel a, arrows). Histological analysis of E12.5, E14.5, and E16.5 embryos also revealed smaller lenses, and frequent persistence of the lens stalk (Fig. 1B, panels e, e', h, h', k arrowheads) and hyaloid vasculature (Fig. 1B, panels h, k open arrowheads) (42.8% of embryos analyzed) (n=21). In the remaining *Ehd1-null* embryos (57.1%), the lens was absent

(aphakia) and the retina misfolded (Fig. 1B, panels f, f', i, i', l, see asterisk) in contrast to controls (Fig. 1B, panels d, d', g, g', j) (n=26). Persistent lens stalk and hyaloid vasculature was also seen in some of the *Ehd1-het* embryos (supplementary Fig. S2). At postnatal day 10 (P10), control eyes consisted of a well-formed lens with an overlying cornea and a laminated retina (Fig. 1B, panels m, m'). In contrast, *Ehd1-null* mice of the same age exhibited eyes phenotypes ranging from a near normal lens, cornea and retina (Fig. 1B, panels n, n') to absent lens and misfolded retina (Fig. 1B, panel o, o', see asterisk). Together, these results indicated that EHD1 is necessary for proper differentiation of ocular tissues including the lens, cornea and retina. In this report, we have focused on the impact of *Ehd1* deletion on lens and corneal development. The effects of *Ehd1* loss on retinal development will be described separately.

EHD1 is expressed in the developing eye

All EHD mRNAs are known to be expressed in developing lens epithelial cells as demonstrated by a transcriptomic study of laser capture micro-dissected surface ectoderm of the E9.5 lens placode (Huang et al., 2011). We performed immunofluorescence studies to assess endogenous expression of EHD1 protein in ocular tissues. EHD1 expression was localized in the apical junctions of epithelial cells lining the lens pit, and in the underlying optic cup at E10.5 (Fig. 2A); EHD1 staining partly colocalized with the adherens junctional marker, E-cadherin (Fig. 2B), as seen in merged images (Fig. 2C, arrows). At E12.5, EHD1 was localized to the sub-membranous region of epithelial cells in the lens vesicle, especially under the apical surface (Fig. 2G, I). At E14.5, EHD1 expression was seen in the lens epithelial and fiber cells, the periocular mesenchymal cells that would form the future corneal stroma and endothelial layers (Fig. 2M, O). Expression of EHD1 was detectable in the lens, corneal epithelial, corneal endothelial cells at E16.5 (Fig. 2U, W). In late postnatal eyes, EHD1 was also expressed in the ganglion cell layer and the outer and inner nuclear layers of the neural retina (data not shown), consistent with a previous report (Rapaport et al., 2006). Loss of EHD1 expression in *Ehd1-null* embryos was confirmed by immunofluorescence (Fig. 2D, F, J, L, P, R, X, Z, arrowheads). These results correlated the ocular phenotypes seen in *Ehd1-null* embryos with loss of EHD1 expression in these tissues.

Our previous studies have demonstrated that deletion of individual EHD family members often results in the up-regulation of other family members in various organ systems compensating for the loss of function of the deleted gene (George et al., 2010; George et al., 2011; Gudmundsson et al., 2010; Rainey et al., 2010). To assess if the loss of EHD1 expression in ocular tissues led to up-regulation of expression of other EHD proteins, we examined the expression levels of EHD2, EHD3 and EHD4 in ocular tissues of *Ehd1-null* and WT mice. At E12.5, the highest EHD2 expression within the eye was seen in the surface ectoderm (Fig. 3A, arrows), blood vessels in the vitreous, the optic cup (Fig. 3A), and in RPE cells surrounding the neural retina in WT (Fig. 3A, arrows) as well as in *Ehd1-null* embryos (Fig. 3B arrowheads). At E16.5, EHD2 expression was observed in the corneal and eyelid epithelium (Fig. 3C, arrows) in WT and *Ehd1-null* eyes (Fig. 3D, arrowheads). Ubiquitous expression of EHD3 and EHD4 was seen in all ocular tissues at E12.5 and at E16.5 (Fig. 3E, G, G' and I, K, K' arrows). EHD2 and EHD3 expression in *Ehd1-null* ocular tissues remained unaltered (Fig. 3F, H, H' and J, L, L' arrowheads). EHD4 expression,

though unaltered in the *Ehd1-null* embryos at E12.5 (Fig. 3J), was reduced in the lens epithelial cells (Fig. 3L, L', arrowheads). These results suggested that, a) EHD proteins show overlapping expression patterns during early ocular development and b) the lack of compensatory upregulation of EHD2–4 expression in *Ehd1-null* eyes suggest unique functions of EHD1 in regulating eye development. It should be noted that *Ehd3-null* or *Ehd4-null* embryos do not show any ocular abnormalities.

As lens development was altered in *Ehd1-null* embryos, we performed immunofluorescence (IF) studies to assess the expression of two genes critical for early lens differentiation in these mutants. The paired domain and homeodomain-containing transcription factor Pax6 and the high mobility group (HMG) domain transcription factor Sox2 are required for specification of lens ectodermal precursors (Ashery-Padan and Gruss, 2001; Ogino et al., 2012). Heterozygous mutations in Pax6 gene are associated with ocular abnormalities including *Aniridia* and Peter's anomaly in humans (Glaser et al., 1994), and *Small eye* phenotype in mice and rats (Hill et al., 1991; Hogan et al., 1986). In addition, Pax6 overexpression or loss-of-function mutations results in microphthalmia or anophthalmia (Schedl et al., 1996). Sox2 mutations in humans result in severe anophthalmia and microphthalmia (Fantes et al., 2003; Hagstrom et al., 2005). Conditional deletion of *Sox2* results in a failure of lens vesicle formation, with reduced expression of β-crystallin and Prox1 expression. In *Ehd1-null* eyes, Pax6 and Sox2 expression and localization were comparable to WT controls (supplementary Fig. S3). These results indicated that the lens developmental defects seen in the *Ehd1-null* lenses were not due to altered Pax6 or Sox2 expression.

Conditional deletion of EHD1 in the lens leads to microphthalmia and cataracts

Embryonic eye development in mice begins during late gastrulation at E9.5, when neuroepithelium derived from the diencephalon evaginates bilaterally to form the optic vesicle (OV). The OV makes contact with a layer of surface epithelium termed presumptive lens ectoderm (PLE): this ectoderm thickens to form the lens placode. As the OV and surface epithelium associate closely through the formation of cytoplasmic extensions, inductive signaling between them shapes each other's subsequent development (Robinson, 2006). In the *Ehd1-null* mice, EHD1 expression is lost not only in the lens but also in surrounding ocular tissues such as optic vesicle (and later retina) that are necessary for early lens differentiation. Therefore, in order to determine whether alterations in lenticular development in *Ehd1-null* mice is due to loss of EHD1 in the lens, we generated conditional knockout mice with *Ehd1* deleted in the lens. The *Le-Cre* transgenic line expresses Cre downstream of a 6.5 Kb genomic fragment derived from the mouse Pax6 promoter that activates Pax6 expression in the surface ectodermal cells that differentiate into corneal and conjunctival epithelial cells, and the pancreas (Ashery-Padan et al., 2000b). Thus, *Le-Cre* mediated deletion is observed in the surface ectoderm-derived tissues including the lens, cornea, conjunctival epithelium and eyelids, as expected. Mating the $Ehd1^{flox/flox}$ mice (Rainey et al., 2010) to the *Le-Cre* transgenic mice allowed us to conditionally delete *Ehd1 (CKO)* in the lens and ocular surface epithelial cells (cornea, conjunctiva, eyelids) (Ashery-Padan et al., 2000a) (Fig. 4A).

The GFP reporter within the *Le-Cre* transgene, which served as a surrogate for Cre expression, was expressed at E11.5 in the lens vesicle in *Ehd1 CKO* (Fig. 4C). PCR analysis of tail DNA also confirmed the genotypes of the *Ehd1 CKO* and control mice (data not shown). *Ehd1 CKO* mice were born at the expected Mendelian ratios. Immunofluorescence studies showed the loss of EHD1 expression in the lens, cornea and conjunctival epithelial cells but not in the optic cup or retina of *EHD1 CKO* embryos (Fig. 4E, G, I, arrowheads) compared to control embryos (Fig. 4D, F, H, arrows) directly correlating Cre expression with loss of EHD1 expression.

Similar to *Ehd1-null* mice, adult Ehd1 CKO (6 weeks or older) mice also displayed microphthalmia and cataracts (supplementary Fig. S4). Nearly 80% of *Ehd1 CKO* animals exhibited ocular phenotypes with microphthalmia (41.6%) and cataracts (23.2%) and microphthalmia together with cataracts (15.5%) (Table 2). Our experimental crosses were set to compare control mice with Le-Cre; $Ehd1^{flox/flox}$ or $Ehd1^{flox/+}$ strains. We observe ocular phenotypes (including microphthalmia and cataracts) in $Ehd1^{flox/+}$.*Le-Cre* mice but this is seen in a smaller proportion of mice (Table 3) compared to defects in $Ehd1^{flox/flox}$.*Le-Cre* mice (Table 2). Out of 62 eyes analyzed for the $Ehd1^{flox/+}$.*Le-Cre* genotype, 35 were affected by either microphthalmia or cataracts (56.45 %)(Table 3). We also observed lens defects in $Ehd1^{+/-}$ whole body mice, again at a lower frequency (numbers not recorded) compared to $Ehd1^{-/-}$ mice (Table 1). Although we have not carried out detailed studies comparing *Le-Cre* allele on a mixed B6.FvB background to our experimental mice, given the reported effects of *Le-Cre* allele itself on lens development (Dora et al., 2014), it is possible that a modifier gene on C57Bl/6 background amplifies the *Le-Cre* effect. However, our results using a total body *Ehd1* deletion support the conclusion that defects upon *Le-Cre*-mediated heterozygous or homozygous *Ehd1* deletion are largely a result of loss of *Ehd1*.

Interestingly, though the proportion of mice with ocular abnormalities was higher in the *Ehd1 CKO* compared to whole body *Ehd1-null* mice, the *CKO* mice exhibited a less severe phenotype and anophthalmia was not observed in *Ehd1 CKO* mice. These results support a lens-intrinsic role for *Ehd1*, but also suggest that loss of *Ehd1* in non-lens tissues enhances the severity of lens defects seen in whole body *Ehd1-null* mice. Overall, these results confirm the requirement of *Ehd1* for early lens development. Since *Ehd1 CKO* mice recapitulated the major lens phenotypes observed in *Ehd1-null* mice further cellular and molecular characterization were carried out using these mice.

Histological characterization of defective lens development in *EHD1 CKO* mice

Histological examination of H&E sections revealed alterations in the development of *Ehd1 CKO* lenses (Fig. 5A, panels a – i'). At E10.5, the lens ectoderm in control embryos had invaginated to form the lens pit (Fig. 5A, panel a, arrow), which had deepened to form a lens vesicle by day E11.5. The lens pit and vesicle, though smaller, were still seen at similar ages in the *Ehd1 CKO* embryo (Fig. 5A, panel b, arrowhead), suggesting that *Ehd1* deletion does not affect lens induction, invagination or vesicle formation. At E12.5 and E14.5, *Ehd1 CKO* lenses retained their normal polarity and architecture (Fig. 5A, panels d, f), but were smaller than in control animals (Fig. 5A, panels c, e). The lens phenotypes in *Ehd1 CKO* eyes were

accentuated by E16.5 (Fig. 5A, panels h, h', i, i',); the overall lens size was reduced, the epithelial layer of lenses was invariably thinner with sparse cells (Fig. 5A, panels i, i', open arrowheads) (supplementary Fig. S5A) and the corneal endothelium was absent (Fig. 5A, panels i, i', arrowheads). In Z-stacks analysis of DAPI stained nuclei; the *Ehd1 CKO* epithelial nuclei appear smaller and less elongated (supplementary Fig S5 panels B, C). A small proportion (21.4%, n=14 at E16.5) of *Ehd1 CKO* embryos also exhibited the persistence of lens stalks (data not shown). Six months old adult *Ehd1 CKO* mice exhibited highly vacuolated lenses (Fig. 5A, panels k, l, arrows) in contrast to control (Fig. 5A, panel j, arrows). Thus, impaired lens development seen in *Ehd1 CKO* mice reflects a requirement of EHD1 during early lens development. As expected, retinal development appeared unaltered in *Ehd1 CKO* eyes at all stages examined.

During normal eye development, the lens grows by a coordinated balance between lens epithelial cell proliferation and fiber cell differentiation. In response to an inductive signal from the retina, lens epithelial cells near the equator withdraw from the cell cycle, elongate and differentiate as secondary lens fiber cells. This anterior-posterior polarity of the lens is maintained throughout life (Robinson, 2006). In order to determine whether *Ehd1 CKO* lenses remained smaller as a consequence of reduced lens epithelial number, we compared the lens epithelial cell counts between *Ehd1 CKO* and control ($Ehd1^{flox/flox}$) lenses. In control eyes, the epithelial cell numbers steadily increased from E12.5 to E16.5; and were 69.6 ± 4.7, 135.6 ± 6.1 and 186.7 ± 9.4 cells at E12.5, E14.5 and E16.5, respectively ($n \leq 4$). In contrast, the epithelial cell numbers at these stages were 61.3 ± 3.7, 87.1 ± 18.7 and 79.7 ± 2.7 indicating that the lens growth was significantly reduced in *Ehd1 CKO* lenses ($n \leq 5$) (Fig. 5B). In order to assess whether reduced lens epithelial cell number in *Ehd1 CKO* eyes is due to reduced cell proliferation, we performed BrdU incorporation studies. These studies revealed a reduction in BrdU incorporation in *Ehd1 CKO* mice compared to controls at E12.5 ($p < 0.01$) but not at E14.5 or E16.5 (Fig. 5C). These results suggested that the reduced lens size in *Ehd1 CKO* embryos could be, at least in part, due to reduced lens epithelial cell proliferation.

In order to determine if reduced lens epithelial cell number in *Ehd1 CKO* embryos may be due to defects in lens epithelial viability, we performed a TUNEL assay (Fig. 6). An increase in the number of TUNEL-positive nuclei was seen in *Ehd1 CKO* lenses when compared to controls at E10.5, E12.5, E14.5 and E16.5 (Fig. 6 A–J). In addition, increased apoptotic nuclei were observed in adult *Ehd1 CKO* lenses (Supplementary Fig. S6). Since the proliferation rate remained approximately similar between *Ehd1 CKO* and control embryos at E14.5 and E16.5, while more apoptotic cells were seen in the former, the reduced lens epithelial cell numbers in *Ehd1 CKO* at these developmental stages likely arise from increased cell death. The apoptotic cells were more abundant in the periphery, an area reported previously to show the highest expression of FGF receptors (Garcia et al., 2005). However, we have not observed any changes in the activation of FGFR signaling effectors such as phosphorylated ERK or FGF-target genes such as Erm and Er81 (ETS transcription factors) (data not shown), although a detailed characterization of FGF receptors themselves has not been performed. These results suggest that EHD1 is also required for cell survival during early lens development. Together, our results suggest that the smaller lenses seen in

Ehd1 CKO embryos likely arise from a combination of reduced proliferation and increased death of lens epithelial cells.

Aberrant lens epithelial cell polarity but normal fiber cell differentiation in *Ehd1 CKO* embryonic lenses

To assess if the *Ehd1 CKO* lens epithelial cells retained lens epithelial cell characteristics, expression of key epithelial cell polarity markers was examined. In the mature lens, the adherens junctional protein E-cadherin is expressed on the basolateral surfaces of lens epithelial cells but not in lens fiber cells. N-cadherin expression, on the other hand, is present both in the lens epithelium and fiber cells (Pontoriero et al., 2009). At E16.5, immunofluorescence analyses for E-cadherin protein expression revealed that its membrane localization within the cells remained unaffected; however the expression appeared discontinuous (or gaps were observed) in between the lens epithelial cells of *Ehd1 CKO* embryos (Fig. 7B, D, arrowheads). This discontinuous expression is likely due to the reduced lens epithelial cell count. N-cadherin expression pattern and localization remained unchanged in *Ehd1 CKO* vs. control embryonic lenses (Supplementary Fig. S7). The tight junction marker ZO-1 is expressed in tight junctions near the apical surface of lens epithelial cells and elongating fiber cells. ZO-1 staining and gamma-tubulin puncta define the normally formed interface between lens epithelial and fiber cells (Sugiyama et al., 2009). This interface was much shorter and irregular in the *Ehd1 CKO* embryonic lenses (Fig. 7F, H, arrowheads), suggesting a defect in the lens epithelial fiber interface.

Lens fiber cell differentiation is accomplished by proliferating lens epithelial cells giving rise to secondary fiber cells, a process characterized by temporally and spatially regulated expression of crystallins (Cvekl and Duncan, 2007). To determine if the secondary fiber cell differentiation was aberrant, we assessed the expression of lens specific crystallins by immunofluorescence. No discernible differences between control and *Ehd1 CKO* embryonic lenses were observed in the expression pattern of α, β and γ- crystallin proteins at day E16.5 (Supplementary Fig. S8). These results indicate that EHD1, though required for lens epithelial proliferation and survival, appears to be dispensable for crystallin expression.

EHD1 deletion in the lens results in aberrant corneal endothelial differentiation

During mouse embryonic development, corneal endothelium is derived from migrating periocular mesenchymal cells of neural crest and mesodermal origins (Kao et al., 2008). Absence of corneal endothelium was a consistent phenotype seen in *Ehd1 CKO* eyes. To further investigate the alterations in corneal development, we performed a series of immunofluorescence analyses (Fig. 8A–H). We examined the corneal epithelium since *Le-Cre* mediated deletion is also observed in this cell layer, as expected. The expression of Keratin 12 (K12), a marker of early corneal epithelial differentiation, was unaltered in *Ehd1 CKO* (Supplementary Fig. S9), suggesting that EHD1 is not necessary for early corneal epithelial differentiation. The periocular mesenchymal cells that migrate to the anterior segment differentiate as corneal endothelial cells and convert from a mesenchymal to an epithelial state. Though the expression of tight junction protein ZO-1 is not restricted to corneal endothelial cells, its expression in these cells does indicate successful mesenchymal to epithelial transition. We have therefore used ZO-1, a critical component of tight

junctional complexes, here as a marker to assess the corneal endothelial differentiation. Expression of ZO-1 was discontinuous and reduced in the anterior chamber of *Ehd1 CKO* (Fig. 8B, D, arrowheads) compared to control embryos (Fig. 8A, C, arrowheads) at E16.5. We have also used another corneal endothelial differentiation marker, N-cadherin (Beebe and Coats, 2000). Though a proper corneal endothelium had not formed in *Ehd1 CKO* eyes, the disorganized group of mesenchymal cells seen anterior to the lens expressed N-cadherin (Fig. 8F, H, arrowheads). The immunofluorescence data support the results of our histological analyses that corneal endothelial differentiation is indeed compromised. These results suggest that extra-ocular mesenchymal cells that form the corneal endothelial layer failed to develop tight junctions with their neighboring cells, which in turn suggested a failure of the transition from mesenchymal to epithelial state in *Ehd1 CKO* lenses.

Discussion

Endocytic traffic is a key biological process in all eukaryotes. Yet little is known about the physiological roles of endocytic pathways, in particular the recycling arm of endocytic traffic, in regulating tissue morphogenesis in mammals. Endocytic recycling plays an essential role in efficient retrieval, polarization and maintenance of membrane receptors following endocytic internalization (Doherty and McMahon, 2009). The physiological roles of the recently identified EHD family of endocytic regulators are just beginning to be elucidated. Here, by deleting the EHD family member *Ehd1* in the murine germline and in the lens, we demonstrate that EHD1 is a required regulator of lens development in mice. We show that a significant proportion of germline *Ehd1-null* mice display marked ocular abnormalities. These phenotypes included anophthalmia, aphakia, microphthalmia and congenital cataracts. These defects were evident by weaning age and persisted throughout life. To our knowledge, this is the first report implicating endocytic trafficking protein EHD1 in ocular development. Interestingly, loss-of-function mutations of *TBC1D20*, a GTPase-activating protein (GAP) for RAB1 and RAB2 has been linked to *blind sterile* (*bs*) phenotype in mice (Liegel et al., 2013; Park et al., 2014). The *bs* mice exhibit nuclear cataracts and male infertility (Varnum, 1983). Phenotypic characterization of *bs* lens at E17.5 revealed lens abnormalities including reduced lens size and degenerated nuclear fibers that were TUNEL (+)(Liegel et al., 2013).The striking difference between *Ehd1* mutant mice vs *bs* mice is that the lens epithelium is primarily affected in *Ehd1* mutants whereas *bs* mutants exhibit lens degeneration due to defects in fiber cell maturation. Nonetheless, the phenotypic similarities observed between the two mutants suggest a functional relationship between the two genes. It will be of interest to examine if Tbc1d20 or Rab1/Rab2 function together with EHDs in the same pathway or are part of a parallel pathway of endocytic recycling regulation. Warburg micro syndrome (WARBM) is an autosomal recessive disorder characterized by eye, brain, and endocrine abnormalities with loss-of-function mutations in *RABGAP1*, *RABGAP2*, *Rab18* and *TBC1D20*. EHD1 was previously linked to Bardet-Biedl Syndrome (BBS, an autosomal recessive condition with clinical features including retinitis pigmentosa, polydactyly, obesity and mental retardation) loci; however no disease-causing mutations were identified (Haider et al., 1999).

EHD1 expression was seen in the lens, retina and ocular surface epithelia including the cornea and conjunctiva. The other family proteins, EHD2–4 showed overlapping expression

with EHD1 in ocular tissues. EHD proteins are highly similar in structure and exhibit shared as well as unique functions (George et al., 2007) and loss of one EHD family member is usually compensated by upregulation of another (George et al., 2010; George et al., 2011; Mate et al., 2012; Sengupta et al., 2009). Since only about half of *Ehd1-null* animals showed eye phenotypes, we first examined if other EHD family members compensated for loss of EHD1. However, our results did not reveal any increases in EHD2, EHD3, or EHD4 expression even in severely affected *Ehd1-null* eyes. Consistent with a lack of compensation by family members, germline deletion of *Ehd3* or *Ehd4* did not produce any apparent ocular abnormalities (George et al., 2011)(the impact of *Ehd2* deletion has not been determined to date). In contrast, *Ehd1* deletion produces dramatic eye phenotypes that appear very early during embryogenesis and persist throughout life. Altogether, these results suggest that EHD1 plays a dominant role in ocular development, and EHD2–4 expression is insufficient to compensate for the loss of EHD1. It remains possible however that EHD family members, or alternate endocytic pathway regulators, do provide redundancy accounting for apparently normal ocular development in a subset of *Ehd1-null* and *Ehd1 CKO* mice and the strain-dependence of *Ehd1-null* phenotype.

A lens intrinsic role for EHD1

As germline deletion of *Ehd1* exhibited multiple defects including high pre-natal mortality (Rainey et al., 2010), we considered the possibility that ocular abnormalities observed in these mutants could be a secondary consequence of loss of *Ehd1* in other tissues that help regulate eye development. Additionally, even within ocular tissues, development is intimately linked to reciprocal signaling between various compartments, such as those between the developing lens, ocular mesenchyme and optic vesicle (Cvekl and Ashery-Padan, 2014; Donner et al., 2006; Lang, 2004). To test this possibility, we deleted *Ehd1* in cells derived from the ocular surface ectoderm such as lens, corneal and conjuctival epithelial cells. As expected, other alterations seen in the germline deletion of *Ehd1* such as male sterility and embryonic lethality were absent in *Ehd1 CKO* mice. The *Ehd1 CKO* mice recapitulated the lenticular abnormalities such as microphthalmia and cataracts (anophthalmia was distinctly absent) seen in the *Ehd1-null* mice. These results point to a lens-intrinsic role of *Ehd1*. Histological analysis revealed microphthalmic lenses and thinner lens epithelial cells with profound defects in epithelial nuclei. It is interesting to note that EHD1, together with its interaction partner Molecule Interacting with CasL like-1 (MICAL-L1), were recently shown to regulate the process of mitosis. The knockdown of EHD1 and MICAL-L1 in HeLa cells resulted in cytokinesis failure and generation of bi-nucleated and multi-nucleated cells (Reinecke et al., 2015). It will be of interest to assess the role of EHD1 together with its interaction partner MICAL-L1 in cell cycle regulation of lens epithelial cells. Ocular phenotypes in *Ehd1 CKO* were evident at birth and became more pronounced by the weaning age. Although milder compared to those in *Ehd1-null* mice, the ocular phenotypes in *Ehd1 CKO* mice were observed at a higher frequency (135 out of 168 eyes analyzed in *Ehd1 CKO* vs. 119 out of 212 eyes analyzed in *Ehd1-null*). One reason for the increased severity of ocular phenotypes in *Ehd1-null* mice could be the loss of EHD1 in the retina and in periocular mesenchymal cells. Another reason could be differences in genetic background between *Ehd1 CKO* (129.B6.FVB) and *Ehd1-null* (129.B6) mice. Consistent with this possibility is the result that knockout mice enriched for 129Sv/Ev and Swiss

Webster background were apparently normal (Rapaport et al., 2006) whereas *Ehd1-null* mice on 129.B6 background exhibit marked developmental defects, including reduced pre-natal viability, small size, male infertility and ocular defects (Rainey et al., 2010). It should be noted that the two possibilities i.e. lens-intrinsic role for *Ehd1* and influence of genetic background are not mutually exclusive.

EHD1 and lens growth

Though smaller lens pits and vesicles were seen in the *Ehd1 mutants*, the fact that lenses do form suggest that *Ehd1* is dispensable for initial stages of lens development including lens induction, placode formation and initiation of lens invagination. However, invagination, though initiated, is not completed in *Ehd1 mutants* as the lens vesicle fails to separate from the overlying ectoderm. Though observed in a number of mutants (Chen et al., 2008; Kuracha et al., 2011; Pontoriero et al., 2008) lens vesicle detachment is a poorly understood phenomenon. Interestingly, in spite of the persistence of the lens stalks, the lens epithelial cells in these mutants retain the ability to initiate fiber differentiation and primary and secondary fiber cells form appropriately suggesting that *Ehd1* is dispensable for fiber differentiation.

Ehd1 CKO also showed a reduction in E-cadherin expression and aberrant ZO-1 distribution in the lens epithelial compartment. The defective ZO-1 localization and reduced E-cadherin expression indicates altered apico-basal polarity of lens epithelial cells in *Ehd1 CKO* mice, suggesting a role for EHD1 in maintaining lens epithelial cell polarity. These alterations could be a consequence of increased lens epithelial apoptosis. However, we cannot rule out a direct role for *Ehd1* in regulation of E-cadherin and ZO-1. At the lens epithelial- fiber interface, endocytic structures have been noted by electron microscopy (EM) in the avian lens (Bassnett et al., 1994). While nothing is known about endocytic traffic of ZO-1 or other tight junction proteins in the lens, recent studies in other cell line models reveal an important role of endocytic recycling of other tight junction proteins claudin-1 and claudin-2 in maintaining apico-basal polarity (Dukes et al., 2011; Fletcher et al., 2014; Heller et al., 2010). Thus, EHD1 may regulate endocytic recycling of tight junction proteins. Future studies will explore if EHD1, either directly or through its interacting partners, regulates the endocytic recycling of E-cadherin or ZO-1, or their associated proteins, in the lens epithelium.

Our results suggest that the main function of *Ehd1* in lens development is regulation of lens epithelial survival and viability. *Ehd1 mutant* lens epithelial cells show a significantly higher rate of apoptosis. How EHD1 might regulate cell survival and proliferation is not known, but a number of key cell surface receptors that regulate cell proliferation and survival in the lens epithelium are either known e.g. IGF1-R and β*1*-integrin (Jovic et al., 2007; Rotem-Yehudar et al., 2001) or are potential targets of EHD1 including FGF and BMP receptors. For instance, fibroblast growth factor (FGF) receptor signaling is required for lens epithelial and fiber cell survival (Zhao et al., 2008). Loss of BMPR1a leads to increased apoptosis of lens placodal cells (Rajagopal et al., 2009). IGF1R is widely expressed in the germinative and transitional zones in the lens, and in the developing retina, iris, ciliary body and cornea (Xie et al., 2007). Transgenic mice with overexpressed insulin or IGF-1 show altered lens

growth, and fiber cell differentiation defects (Xie et al., 2007). β*1-integrin CKO* in the lens show disorganized lens epithelium and increased epithelial cell death (Simirskii et al., 2007). Future studies will assess if EHD1 regulates these receptors or others that control cell proliferation, survival and epithelial remodeling during lens development.

EHD1 and corneal development

In addition to lens defects in *EHD1 CKO* mice, we observed profound alterations in corneal endothelial differentiation. Normal corneal endothelial layer exhibits regularly-spaced tight junctions and adherens junctions that are recognized by staining for ZO-1 and N, or E-cadherin, respectively.

In contrast to control embryos, the cells lining the inner surface of corneal stroma in *Ehd1 CKO* embryos failed to form proper junctional complexes, which is evident by the absence of ZO-1 staining of these cells. N-cadherin expression was seen in multiple cell layers in the *Ehd1 CKO* compared to a single layer in control mice. These alterations reflect the failure of the mesenchymal corneal endothelial precursors to convert to an epithelial identity with apico-basal polarity. Though we cannot rule out the possibility of a direct role for *Ehd1* in regulating corneal endothelial differentiation, it is likely that altered corneal endothelial differentiation is due to loss of *Ehd1* in adjacent ocular tissues such as the lens and /or in the corneal epithelial cells. Corneal endothelium phenotype is a non-cell autonomous phenotype as *Le-Cre* deletion does not occur in the mesenchymal and neural crest derived cells. EHD1 expression in the corneal endothelial precursors was unaltered in the *Ehd1 CKO* as the Cre recombinase is not expressed in these cells. Signals from the lens are known to regulate N-cadherin expression in avian eyes (Beebe and Coats, 2000). In addition, ablation of lens in mice inhibits corneal endothelial formation (Zhang et al., 2007). The lens thus serves as a critical signaling center that orchestrates overall development of the corneal endothelium and the stroma (Gage and Zacharias, 2009). A more direct impact of EHD1 in corneal endothelium will be of considerable interest given the ion and water transport functions of this cell layer. The corneal endothelial cells help maintain hydration and in turn, corneal transparency by the expression of Na^+/K^+-ATPase and bicarbonate-dependent Mg^{2+}-ATPase pumps (Bonanno, 2012; Srinivas, 2010). Notably, EHD proteins associate with ankyrin proteins to regulate membrane targeting and stability of membrane ion channels in cardiomyocytes, and lack of EHD3 expression impairs the expression and function of Na/Ca exchanger (NCX) in these cells (Curran et al., 2014; Gudmundsson et al., 2010).

In conclusion, our studies using germline and conditional knockouts of *Ehd1* provide evidence for a novel role of the endocytic recycling pathway in regulating key ocular developmental decisions during mouse lens development. Further studies using this model should help delineate how the basic process of endocytic recycling is intertwined with cell-cell interaction and signaling pathways to regulate developmental decisions in the mammalian eye.

Supplementary Material

Refer to Web version on PubMed Central for supplementary material.

Acknowledgements

We thank Dr. Ashery-Padan (Tel Aviv University, Tel Aviv, Israel) for permission to use the Le-Cre strain and Dr. David Beebe (Washington University in St. Louis) for advice and providing breeding stocks of *Le-Cre* mice. We thank members of the Band Laboratory for discussion and suggestions. PA, SB and BM were recipients of graduate fellowships through the Program of Excellence Graduate Assistantships from UNMC. This work was supported by the NIH grants CA105489, CA87986, CA99163 and CA116552 to HB, CA96844 and CA144027 to VB, and EY017610 to VG; Nebraska Department of Health and Human Services LB506 (2014-01) and LB606 (18123-Y3) grants to HB; Department of Defense grants W81XWH-07-1-0351 and W81XWH-11-1-0171 to VB; and the NCI CCSG to Buffett Cancer Center.

References

Ashery-Padan R, Gruss P. Pax6 lights-up the way for eye development. Curr. Opin. Cell Biol. 2001; 13:706–714. [PubMed: 11698186]

Ashery-Padan R, Marquardt T, Zhou X, Gruss P. Pax6 activity in the lens primordium is required for lens formation and for correct placement of a single retina in the eye. Genes Dev. 2000a; 14:2701–2711. [PubMed: 11069887]

Ashery-Padan R, Marquardt T, Zhou X, Gruss P. Pax6 activity in the lens primordium is required for lens formation and for correct placement of a single retina in the eye. Genes Dev. 2000b; 14:2701–2711. [PubMed: 11069887]

Bassnett S, Kuszak JR, Reinisch L, Brown HG, Beebe DC. Intercellular communication between epithelial and fiber cells of the eye lens. J. Cell. Sci. 1994; 107(Pt 4):799–811. [PubMed: 8056837]

Beebe DC, Coats JM. The lens organizes the anterior segment: Specification of neural crest cell differentiation in the avian eye. Dev. Biol. 2000; 220:424–431. [PubMed: 10753528]

Bokel C, Brand M. Endocytosis and signaling during development. Cold Spring Harb Perspect. Biol. 2014; 6

Bonanno JA. Molecular mechanisms underlying the corneal endothelial pump. Exp. Eye Res. 2012; 95:2–7. [PubMed: 21693119]

Caplan S, Naslavsky N, Hartnell LM, Lodge R, Polishchuk RS, Donaldson JG, Bonifacino JS. A tubular EHD1-containing compartment involved in the recycling of major histocompatibility complex class I molecules to the plasma membrane. EMBO J. 2002; 21:2557–2567. [PubMed: 12032069]

Chen Y, Doughman YQ, Gu S, Jarrell A, Aota S, Cvekl A, Watanabe M, Dunwoodie SL, Johnson RS, van Heyningen V, Kleinjan DA, Beebe DC, Yang YC. Cited2 is required for the proper formation of the hyaloid vasculature and for lens morphogenesis. Development. 2008; 135:2939–2948. [PubMed: 18653562]

Curran J, Makara MA, Little SC, Musa H, Liu B, Wu X, Polina I, Alecusan JS, Wright P, Li J, Billman GE, Boyden PA, Gyorke S, Band H, Hund TJ, Mohler PJ. EHD3-dependent endosome pathway regulates cardiac membrane excitability and physiology. Circ. Res. 2014; 115:68–78. [PubMed: 24759929]

Cvekl A, Ashery-Padan R. The cellular and molecular mechanisms of vertebrate lens development. Development. 2014; 141:4432–4447. [PubMed: 25406393]

Cvekl A, Duncan MK. Genetic and epigenetic mechanisms of gene regulation during lens development. Prog. Retin. Eye Res. 2007; 26:555–597. [PubMed: 17905638]

Daumke O, Lundmark R, Vallis Y, Martens S, Butler PJ, McMahon HT. Architectural and mechanistic insights into an EHD ATPase involved in membrane remodelling. Nature. 2007; 449:923–927. [PubMed: 17914359]

de Beer T, Hoofnagle AN, Enmon JL, Bowers RC, Yamabhai M, Kay BK, Overduin M. Molecular mechanism of NPF recognition by EH domains. Nat. Struct. Biol. 2000; 7:1018–1022. [PubMed: 11062555]

Doherty GJ, McMahon HT. Mechanisms of endocytosis. Annu. Rev. Biochem. 2009; 78:857–902. [PubMed: 19317650]

Donner AL, Lachke SA, Maas RL. Lens induction in vertebrates: Variations on a conserved theme of signaling events. Semin. Cell Dev. Biol. 2006; 17:676–685. [PubMed: 17164096]

Dora NJ, Collinson JM, Hill RE, West JD. Hemizygous le-cre transgenic mice have severe eye abnormalities on some genetic backgrounds in the absence of LoxP sites. PLoS One. 2014; 9:e109193. [PubMed: 25272013]

Dukes JD, Fish L, Richardson JD, Blaikley E, Burns S, Caunt CJ, Chalmers AD, Whitley P. Functional ESCRT machinery is required for constitutive recycling of claudin-1 and maintenance of polarity in vertebrate epithelial cells. Mol. Biol. Cell. 2011; 22:3192–3205. [PubMed: 21757541]

Fantes J, Ragge NK, Lynch SA, McGill NI, Collin JR, Howard-Peebles PN, Hayward C, Vivian AJ, Williamson K, van Heyningen V, FitzPatrick DR. Mutations in SOX2 cause anophthalmia. Nat. Genet. 2003; 33:461–463. [PubMed: 12612584]

Fletcher SJ, Iqbal M, Jabbari S, Stekel D, Rappoport JZ. Analysis of occludin trafficking, demonstrating continuous endocytosis, degradation, recycling and biosynthetic secretory trafficking. PLoS One. 2014; 9:e111176. [PubMed: 25422932]

Gage PJ, Zacharias AL. Signaling “cross-talk” is integrated by transcription factors in the development of the anterior segment in the eye. Dev. Dyn. 2009; 238:2149–2162. [PubMed: 19623614]

Garcia CM, Yu K, Zhao H, Ashery-Padan R, Ornitz DM, Robinson ML, Beebe DC. Signaling through FGF receptor-2 is required for lens cell survival and for withdrawal from the cell cycle during lens fiber cell differentiation. Dev. Dyn. 2005; 233:516–527. [PubMed: 15778993]

George M, Rainey MA, Naramura M, Foster KW, Holzapfel MS, Willoughby LL, Ying G, Goswami RM, Gurumurthy CB, Band V, Satchell SC, Band H. Renal thrombotic microangiopathy in mice with combined deletion of endocytic recycling regulators EHD3 and EHD4. PLoS One. 2011; 6:e17838. [PubMed: 21408024]

George M, Rainey MA, Naramura M, Ying G, Harms DW, Vitaterna MH, Doglio L, Crawford SE, Hess RA, Band V, Band H. Ehd4 is required to attain normal prepubertal testis size but dispensable for fertility in male mice. Genesis. 2010; 48:328–342. [PubMed: 20213691]

George M, Ying G, Rainey MA, Solomon A, Parikh PT, Gao Q, Band V, Band H. Shared as well as distinct roles of EHD proteins revealed by biochemical and functional comparisons in mammalian cells and C. elegans. BMC Cell Biol. 2007; 8:3. [PubMed: 17233914]

Glaser T, Jepeal L, Edwards JG, Young SR, Favor J, Maas RL. PAX6 gene dosage effect in a family with congenital cataracts, aniridia, anophthalmia and central nervous system defects. Nat. Genet. 1994; 7:463–471. [PubMed: 7951315]

Grant B, Zhang Y, Paupard MC, Lin SX, Hall DH, Hirsh D. Evidence that RME-1, a conserved C. elegans EH-domain protein, functions in endocytic recycling. Nat. Cell Biol. 2001; 3:573–579. [PubMed: 11389442]

Grant BD, Donaldson JG. Pathways and mechanisms of endocytic recycling. Nat. Rev. Mol. Cell Biol. 2009; 10:597–608. [PubMed: 19696797]

Grant BD, Caplan S. Mechanisms of EHD/RME-1 protein function in endocytic transport. Traffic. 2008; 9:2043–2052. [PubMed: 18801062]

Gudmundsson H, Hund TJ, Wright PJ, Kline CF, Snyder JS, Qian L, Koval OM, Cunha SR, George M, Rainey MA, Kashef FE, Dun W, Boyden PA, Anderson ME, Band H, Mohler PJ. EH domain proteins regulate cardiac membrane protein targeting. Circ. Res. 2010; 107:84–95. [PubMed: 20489164]

Guilherme A, Soriano NA, Furcinitti PS, Czech MP. Role of EHD1 and EHBP1 in perinuclear sorting and insulin-regulated GLUT4 recycling in 3T3-L1 adipocytes. J. Biol. Chem. 2004; 279:40062–40075. [PubMed: 15247266]

Hagstrom SA, Pauer GJ, Reid J, Simpson E, Crowe S, Maumenee IH, Traboulsi EI. SOX2 mutation causes anophthalmia, hearing loss, and brain anomalies. Am. J. Med. Genet. A. 2005; 138A:95–98. [PubMed: 16145681]

Haider NB, Searby C, Galperin E, Mintz L, Horowitz M, Stone EM, Sheffield VC. Evaluation and molecular characterization of EHD1, a candidate gene for bardet-biedl syndrome 1 (BBS1). Gene. 1999; 240:227–232. [PubMed: 10564830]

Heller B, Adu-Gyamfi E, Smith-Kinnaman W, Babbey C, Vora M, Xue Y, Bittman R, Stahelin RV, Wells CD. Amot recognizes a juxtanuclear endocytic recycling compartment via a novel lipid binding domain. J. Biol. Chem. 2010; 285:12308–12320. [PubMed: 20080965]

Hill RE, Favor J, Hogan BL, Ton CC, Saunders GF, Hanson IM, Prosser J, Jordan T, Hastie ND, van Heyningen V. Mouse small eye results from mutations in a paired-like homeobox-containing gene. Nature. 1991; 354:522–525. [PubMed: 1684639]

Hogan BL, Horsburgh G, Cohen J, Hetherington CM, Fisher G, Lyon MF. Small eyes (sey): A homozygous lethal mutation on chromosome 2 which affects the differentiation of both lens and nasal placodes in the mouse. J. Embryol. Exp. Morphol. 1986; 97:95–110. [PubMed: 3794606]

Huang J, Rajagopal R, Liu Y, Dattilo LK, Shaham O, Ashery-Padan R, Beebe DC. The mechanism of lens placode formation: A case of matrix-mediated morphogenesis. Dev. Biol. 2011; 355:32–42. [PubMed: 21540023]

Jones MC, Caswell PT, Norman JC. Endocytic recycling pathways: Emerging regulators of cell migration. Curr. Opin. Cell Biol. 2006; 18:549–557. [PubMed: 16904305]

Kao WW, Xia Y, Liu CY, Saika S. Signaling pathways in morphogenesis of cornea and eyelid. Ocul. Surf. 2008; 6:9–23. [PubMed: 18264652]

Kieken F, Sharma M, Jovic M, Panapakkam Giridharan SS, Naslavsky N, Caplan S, Sorgen PL. Mechanism for the selective interaction of C-terminal Eps15 homology domain proteins with specific asn-pro-phe-containing partners. J. Biol. Chem. 2010; 285:8687–8694. [PubMed: 20106972]

Kieken F, Jovic M, Naslavsky N, Caplan S, Sorgen PL. EH domain of EHD1. J. Biomol. NMR. 2007; 39:323–329. [PubMed: 17899392]

Kuracha MR, Burgess D, Siefker E, Cooper JT, Licht JD, Robinson ML, Govindarajan V. Spry1 and Spry2 are necessary for lens vesicle separation and corneal differentiation. Invest. Ophthalmol. Vis. Sci. 2011; 52:6887–6897. [PubMed: 21743007]

Lang RA. Pathways regulating lens induction in the mouse. Int. J. Dev. Biol. 2004; 48:783–791. [PubMed: 15558471]

Lee DW, Zhao X, Scarselletta S, Schweinsberg PJ, Eisenberg E, Grant BD, Greene LE. ATP binding regulates oligomerization and endosome association of RME-1 family proteins. J. Biol. Chem. 2005; 280:17213–17220. [PubMed: 15710626]

Liegel RP, Handley MT, Ronchetti A, Brown S, Langemeyer L, Linford A, Chang B, Morris-Rosendahl DJ, Carpanini S, Posmyk R, Harthill V, Sheridan E, Abdel-Salam GM, Terhal PA, Faravelli F, Accorsi P, Giordano L, Pinelli L, Hartmann B, Ebert AD, Barr FA, Aligianis IA, Sidjanin DJ. Loss-of-function mutations in TBC1D20 cause cataracts and male infertility in blind sterile mice and warburg micro syndrome in humans. Am. J. Hum. Genet. 2013; 93:1001–1014. [PubMed: 24239381]

Lin SX, Grant B, Hirsh D, Maxfield FR. Rme-1 regulates the distribution and function of the endocytic recycling compartment in mammalian cells. Nat. Cell Biol. 2001; 3:567–572. [PubMed: 11389441]

Mate SE, Van Der Meulen JH, Arya P, Bhattacharyya S, Band H, Hoffman EP. Eps homology domain endosomal transport proteins differentially localize to the neuromuscular junction. Skelet Muscle. 2012; 2 19-5040-2-19.

Maxfield FR, McGraw TE. Endocytic recycling. Nat. Rev. Mol. Cell Biol. 2004; 5:121–132. [PubMed: 15040445]

Montagnac G, Echard A, Chavrier P. Endocytic traffic in animal cell cytokinesis. Curr. Opin. Cell Biol. 2008; 20:454–461. [PubMed: 18472411]

Naslavsky N, Caplan S. EHD proteins: Key conductors of endocytic transport. Trends Cell Biol. 2011; 21:122–131. [PubMed: 21067929]

Ogino H, Ochi H, Reza HM, Yasuda K. Transcription factors involved in lens development from the preplacodal ectoderm. Dev. Biol. 2012; 363:333–347. [PubMed: 22269169]

Park AK, Liegel RP, Ronchetti A, Ebert AD, Geurts A, Sidjanin DJ. Targeted disruption of Tbc1d20 with zinc-finger nucleases causes cataracts and testicular abnormalities in mice. BMC Genet. 2014; 15 135-014-0135-2.

Pontoriero GF, Smith AN, Miller LA, Radice GL, West-Mays JA, Lang RA. Cooperative roles for E-cadherin and N-cadherin during lens vesicle separation and lens epithelial cell survival. Dev. Biol. 2009; 326:403–417. [PubMed: 18996109]

Pontoriero GF, Deschamps P, Ashery-Padan R, Wong R, Yang Y, Zavadil J, Cvekl A, Sullivan S, Williams T, West-Mays JA. Cell autonomous roles for AP-2alpha in lens vesicle separation and maintenance of the lens epithelial cell phenotype. Dev. Dyn. 2008; 237:602–617. [PubMed: 18224708]

Posey AD Jr, Swanson KE, Alvarez MG, Krishnan S, Earley JU, Band H, Pytel P, McNally EM, Demonbreun AR. EHD1 mediates vesicle trafficking required for normal muscle growth and transverse tubule development. Dev. Biol. 2014; 387:179–190. [PubMed: 24440153]

Rainey MA, George M, Ying G, Akakura R, Burgess DJ, Siefker E, Bargar T, Doglio L, Crawford SE, Todd GL, Govindarajan V, Hess RA, Band V, Naramura M, Band H. The endocytic recycling regulator EHD1 is essential for spermatogenesis and male fertility in mice. BMC Dev. Biol. 2010; 10:37. [PubMed: 20359371]

Rajagopal R, Huang J, Dattilo LK, Kaartinen V, Mishina Y, Deng CX, Umans L, Zwijsen A, Roberts AB, Beebe DC. The type I BMP receptors, Bmpr1a and Acvr1, activate multiple signaling pathways to regulate lens formation. Dev. Biol. 2009; 335:305–316. [PubMed: 19733164]

Rapaport D, Auerbach W, Naslavsky N, Pasmanik-Chor M, Galperin E, Fein A, Caplan S, Joyner AL, Horowitz M. Recycling to the plasma membrane is delayed in EHD1 knockout mice. Traffic. 2006; 7:52–60. [PubMed: 16445686]

Reinecke JB, Katafiasz D, Naslavsky N, Caplan S. Novel functions for the endocytic regulatory proteins MICAL-L1 and EHD1 in mitosis. Traffic. 2015; 16:48–67. [PubMed: 25287187]

Robinson ML. An essential role for FGF receptor signaling in lens development. Semin. Cell Dev. Biol. 2006; 17:726–740.

Russell P, Zigler JS Jr, Reddy V. The development of a monoclonal antibody to a human gamma crystallin. Curr. Eye Res. 1984; 3:1329–1335. [PubMed: 6510011]

Schedl A, Ross A, Lee M, Engelkamp D, Rashbass P, van Heyningen V, Hastie ND. Influence of PAX6 gene dosage on development: Overexpression causes severe eye abnormalities. Cell. 1996; 86:71–82. [PubMed: 8689689]

Scheiblin DA, Gao J, Caplan JL, Simirskii VN, Czymmek KJ, Mathias RT, Duncan MK. Beta-1 integrin is important for the structural maintenance and homeostasis of differentiating fiber cells. Int. J. Biochem. Cell Biol. 2014; 50:132–145. [PubMed: 24607497]

Scita G, Di Fiore PP. The endocytic matrix. Nature. 2010; 463:464–473. [PubMed: 20110990]

Sengupta S, George M, Miller KK, Naik K, Chou J, Cheatham MA, Dallos P, Naramura M, Band H, Zheng J. EHD4 and CDH23 are interacting partners in cochlear hair cells. J. Biol. Chem. 2009; 284:20121–20129. [PubMed: 19487694]

Sharma M, Naslavsky N, Caplan S. A role for EHD4 in the regulation of early endosomal transport. Traffic. 2008; 9:995–1018. [PubMed: 18331452]

Srinivas SP. Dynamic regulation of barrier integrity of the corneal endothelium. Optom. Vis. Sci. 2010; 87:E239–E254. [PubMed: 20142793]

Sugiyama Y, Akimoto K, Robinson ML, Ohno S, Quinlan RA. A cell polarity protein aPKClambda is required for eye lens formation and growth. Dev. Biol. 2009; 336:246–256. [PubMed: 19835853]

Varnum DS. Blind-sterile: A new mutation on chromosome 2 of the house mouse. J. Hered. 1983; 74:206–207. [PubMed: 6863898]

Walseng E, Bakke O, Roche PA. Major histocompatibility complex class II-peptide complexes internalize using a clathrin- and dynamin-independent endocytosis pathway. J. Biol. Chem. 2008; 283:14717–14727. [PubMed: 18378669]

Zhang Y, Overbeek PA, Govindarajan V. Perinatal ablation of the mouse lens causes multiple anterior chamber defects. Mol. Vis. 2007; 13:2289–2300. [PubMed: 18199970]

Highlights

- *Ehd1-mutants* display pleiotropic ocular phenotypes.
- Ocular phenotypes in *Ehd1-mutants* appear during embryonic development.
- Conditional *Ehd1* deletion reveals EHD1 requirement for lens and corneal development.
- *Ehd1* deletion in the lens promotes increased cell death and decreased proliferation.

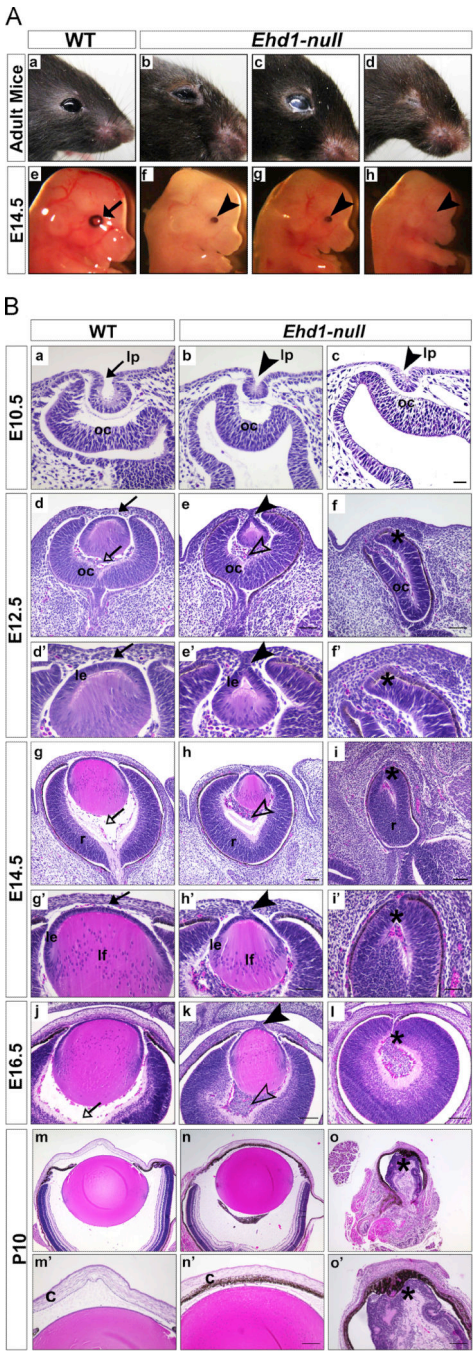

Fig. 1. Defective ocular development in *Ehd1-null* mice

1A: Gross anatomical features of eye structures of *Ehd1-null* adult mice (b, c, d) and E14.5 embryos (f, g, h) were compared to control adult mice (a) and embryos (e). Shown are examples of microphthalmia (b), cataract (c) and anophthalmia (d) in *Ehd1-null* mice. At embryonic day E14.5, smaller eyes and irregular retinal-pigmented epithelium (RPE) are visible in *Ehd1-null* embryos (f, g, h) compared to littermate wild type control (e). **1B:** Histological analyses of formalin-fixed, paraffin-embedded sections depicting examples of: smaller lens pits in *Ehd1-null* (b, c) compared to WT (a) at E10.5; and lens stalk persistence

(e, e’ h, h’, k, arrowheads), hyaloid vasculature persistence (e, e’, h, h’, k, open arrowheads), aphakia (f, f’, i, i’, l, asterisk) in *Ehd1-null* compared to WT controls (d, d’ g, g’ j, arrows) at E12.5, E14.5, E16.5; normal architecture of the lens and the retina with a smaller lens (n, n’) and a severely malformed residual eye in *Ehd1-null* mice (o, o’, asterisk) at P10 vs. a well-formed lens, cornea and distinct lamination of neural retina in WT eyes (m, m’).
Abbreviations: c, cornea; le, lens epithelium; lf, lens fiber; lp, lens pit; oc, optic cup; cells; r, retina. Scale bars are 50 μm in panels (a, b, c, d’, e’, f’, g’, h’, i’), 100 μm in panels (d, e, f, j, k, l, m’, n’, o’) and 200 μm in panels (g, h, i, m, n, o).

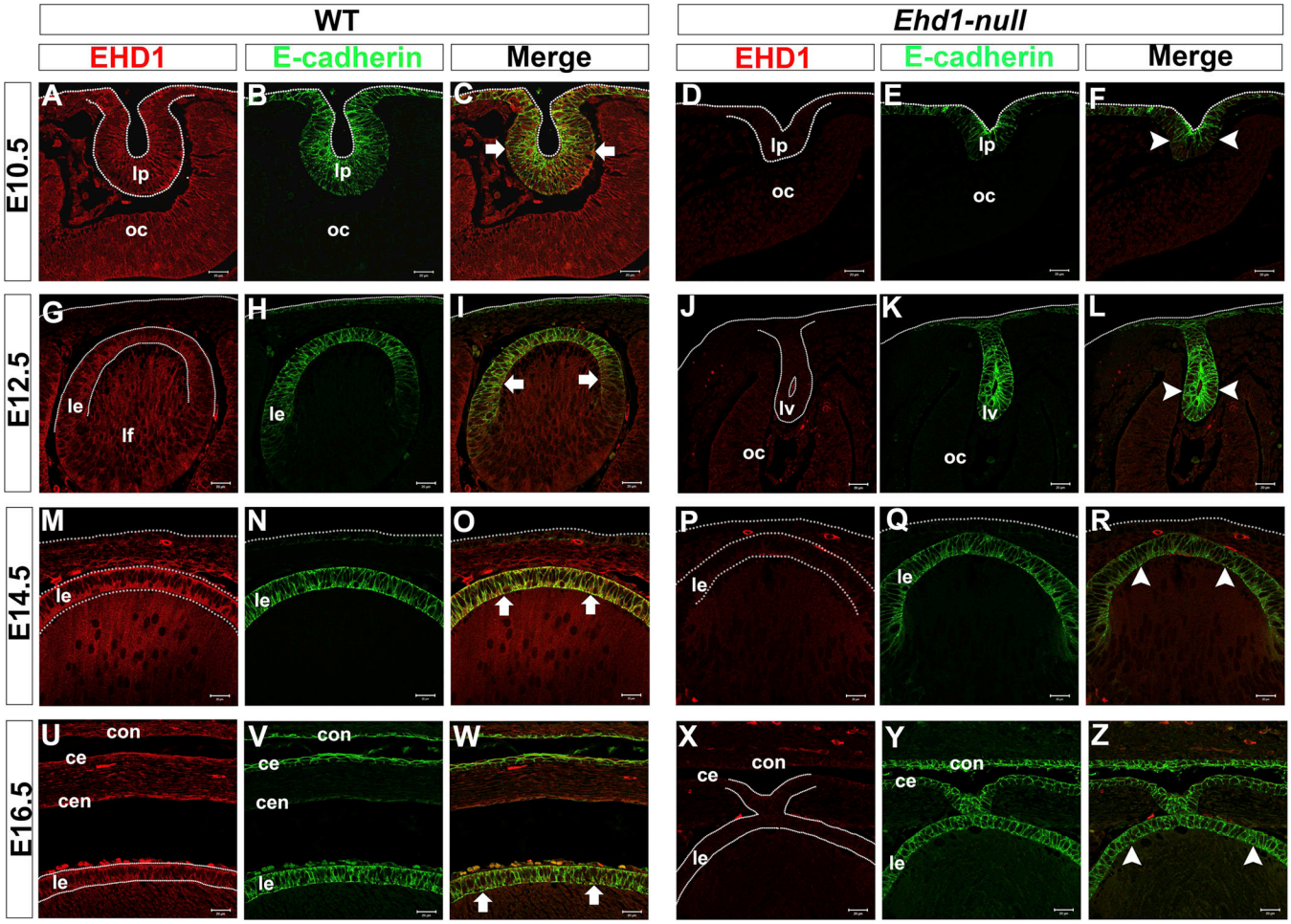

Fig. 2. EHD1 expression during mouse eye development

Formalin-fixed, paraffin-embedded 4 μm thick eye tissue sections, at the indicated embryonic time points, were stained with anti-EHD1 (red) and anti-E-cadherin (green) antibodies and visualized by confocal fluorescence microscopy. In control embryos, EHD1 expression is observed in the lens pit and the underlying optic cup at E10.5 (A, C); in the surface ectoderm, the epithelial cells and the underlying optic cup (G, I) at E12.5; in the overlying ectoderm and the lens epithelial cells (M, O) at E14.5 and in the eyelids, the corneal epithelium, corneal stroma and the lens epithelium (U, W) at E16.5. Colocalization (yellow) is observed along the cells of the lens pit (C, arrows) and the lens epithelium (I, O, W, arrows) in control embryos. EHD1 staining is not observed in *Ehd1-null* at E10.5 (D, F), at E12.5 (J, L), E14.5 (P, R) and E16.5 (X, Z). E-cadherin colocalization with EHD1 is not observed in *Ehd1-null* embryos (F, L, Z, arrowheads). The dotted line demarcates the lens pit, the surface ectoderm and the lens epithelium. Abbreviations: ce, corneal epithelium; cen, corneal endothelium; con, conjunctival epithelium; le, lens epithelium; lf, lens fiber cells; lv, lens vesicle; lp, lens pit; oc, optic cup. Scale bar is 20 μm.

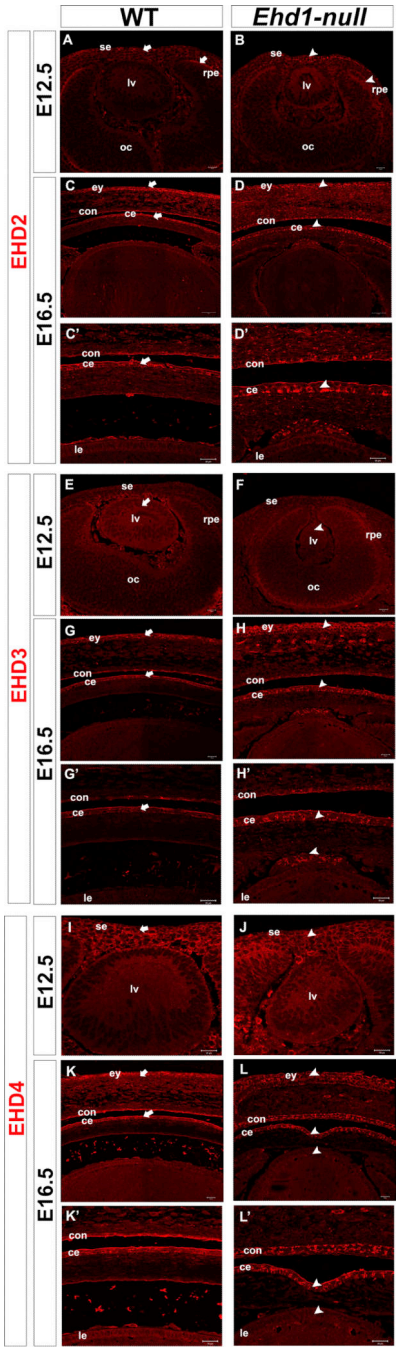

Fig. 3. Expression of EHD family members is not altered in developing eyes of *Ehd1-null* mice

Formalin-fixed, paraffin-embedded tissue sections, at the indicated embryonic time points, were stained with anti-EHD2, anti-EHD3, anti-EHD4 antibodies and visualized by confocal fluorescence microscopy. In control embryos, EHD2 expression is observed in the surface ectoderm (A, arrows), blood vessels of the vitreous, the optic cup (A), the retinal pigmented epithelium (A, arrows) at E12.5 and in the eyelids (C, arrows), the corneal epithelium (C, arrows) at E16.5. EHD2 expression pattern in *Ehd1-null* embryos (B, D, arrowheads) is comparable to that in controls. EHD3 expression is observed in: the overlying surface

ectoderm, the lens vesicle, the optic cup of WT (E) and *Ehd1-null* embryos (F) at E12.5, and in the eyelids, the corneal epithelium, the lens epithelium and surrounding mesenchymal tissues of WT (G, G' arrows) and *Ehd1-null* eyes (H, H' arrowheads). Similarly, EHD4 expression is seen in: the surface ectoderm and lens vesicle of WT (I, arrow) and *Ehd1-null* embryos (J, arrowhead) and in the eyelids, corneal epithelium and in the lens epithelium at E16.5 in WT (K, K' arrow) and *Ehd1-null* (L, L' arrowheads). Abbreviations: ce, corneal epithelium; cen, corneal endothelium; con, conjunctival epithelium; ey, eyelids; le, lens epithelium; lp, lens pit; lv, lens vesicle; oc, optic cup; rpe, retinal pigmented epithelium; se, surface ectoderm. Scale bar is 50 μm in panels C, D and 20 μm in the remaining panels.

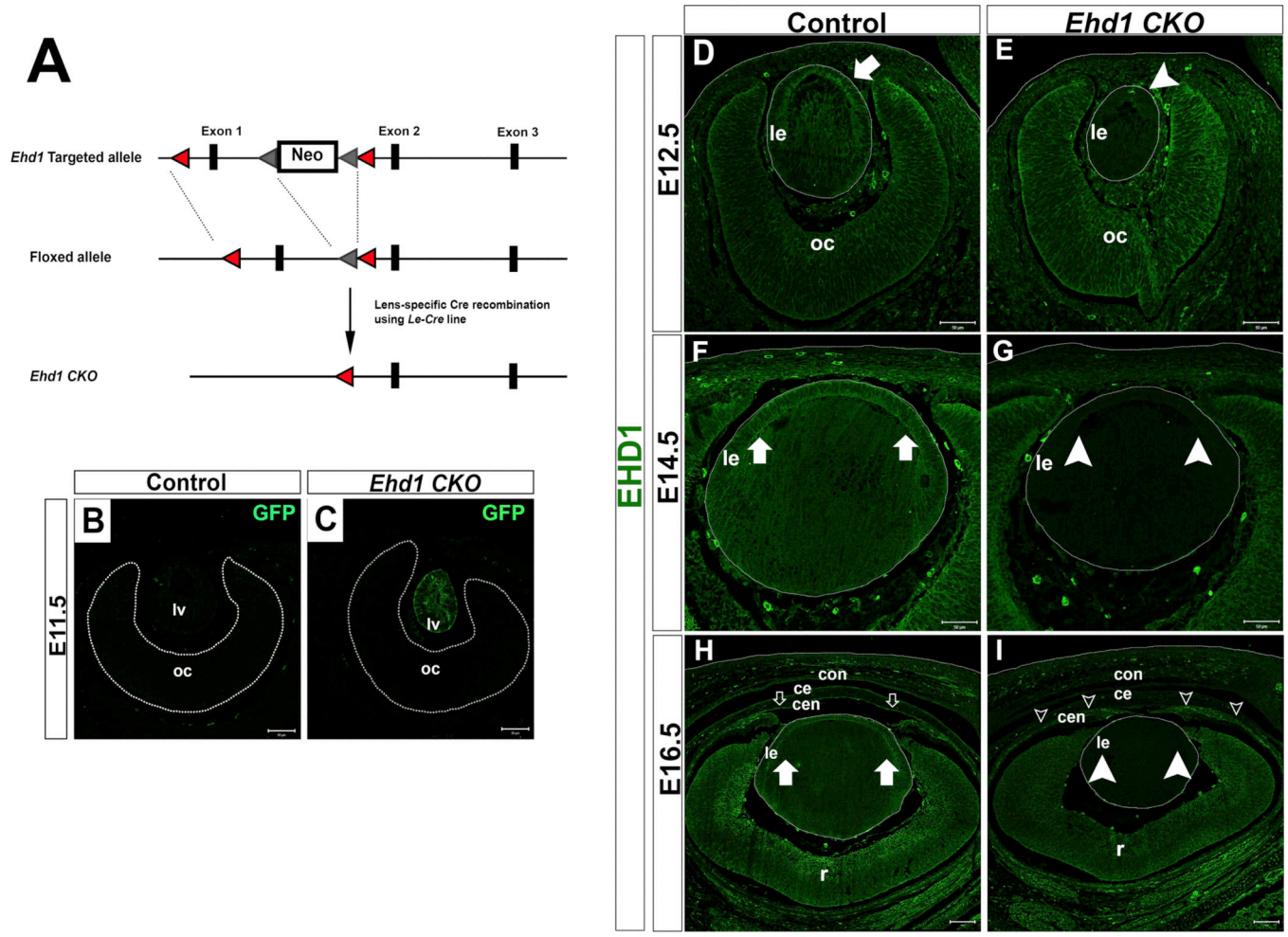

Fig. 4. Conditional deletion of *Ehd1* in the mouse lens

A: Schematic of the floxed *Ehd1* allele with a Neo cassette surrounded by FRT recombination sites (grey triangles) and loxP recombination sites surrounding exon 1 (red triangles) (top), floxed allele after genetic transgenic FLP recombinase-mediated removal of the Neo cassette (middle) and the mutant allele lacking exon 1 sequences (called *Ehd1 CKO*) expected to be generated upon *Le-Cre* driven Cre recombinase expression (bottom). **B, C:** Formalin-fixed paraffin-embedded sections of E11.5 embryonic eyes of control (B; floxed mice lacking *Le-Cre*) or *Ehd1 CKO* mice (C) were subjected to staining with anti-GFP antibody (green) followed by confocal imaging. Lens-specific expression of GFP in *Ehd1 CKO* mice confirms the specificity of *Le-Cre* transgene in our stocks. **D-I:** Control sections (D, F, H) or *Ehd1 CKO* (E, G, I) embryonic eyes at the indicated ages were stained with an anti-EHD1 antibody and analyzed by confocal microscopy. Loss of EHD1 staining is seen specifically in the developing lens in *Ehd1 CKO* embryos (E, G, I, arrowheads) while staining in retina is intact and comparable to that in control embryos (D, F, H). EHD1 expression is also retained in the neural crest derived corneal endothelial cells as seen in E16.5 *Ehd1 CKO* (I, open arrowheads) vs. control (H, open arrows) embryos. A dotted line demarcates the lens boundary in panels D, E, F, G, H, I. Abbreviations: ce, corneal epithelium; cen, corneal endothelium; con, conjunctival epithelium; le, lens epithelium; lv,

lens vesicle; oc, optic cup; r, retina. Scale bar is 50 μm in panels B-G and 100 μm in panels H, I.

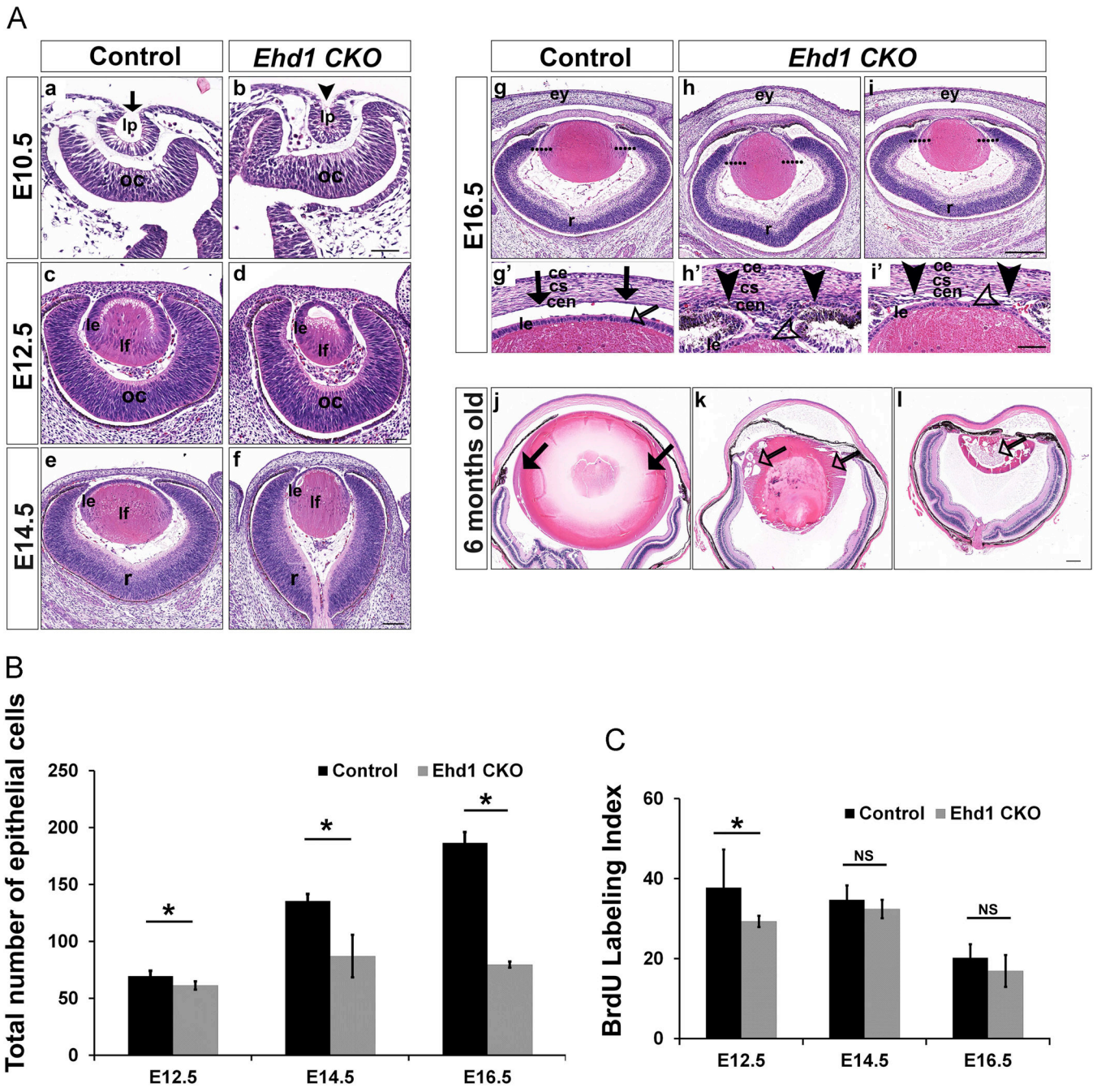

Fig. 5. Lens development defects in *Ehd1 CKO* mice

A: H & E sections of embryonic (a–i) or 6-month old (j–l) eyes from control (a, c, e, g, g', j) or *Ehd1 CKO* mice (b, d, f, h, i, h', i', k, l) at E10.5 (a, b), E12.5 (c, d), E14.5 (e, f), E16.5 (g–i) and 6-months of age (j–l). Smaller lens pit in E10.5 *Ehd1 CKO* (b, arrowhead) compared to control (a, arrow) embryo is indicated. Smaller lenses are seen in *Ehd1 CKO* embryos at E12.5 (d), E14.5 (f) and E16.5 (h, i, h', i'). At E16.5, *Ehd1 CKO* embryonic lenses show lens epithelial thinning, aberrant epithelial cell shape (open arrowheads), and absence of corneal endothelium (downward arrowheads). Open arrows in (panels k, l) represent vacuolated lenses in adult *Ehd1 CKO* mice. The dotted lines on two sides of lens

in panels g-i represents the equator region. g', h', i' panels are higher magnification images of segments from g, h and i panels, respectively. Abbreviations: ce, corneal epithelium; cs, corneal stroma; cen, corneal endothelium; ey, eyelids; le, lens epithelium; lf, lens fiber cells; lp, lens pit; oc, optic cup; r, retina. Scale bar is 100 μm. **B:** Lens epithelial cell numbers in control (black bars) and *Ehd1 CKO* eyes (grey bars) at E12.5, E14.5, E16.5 were quantified and performed as described in Methods. Error bars indicate SEM. *$p < 0.001$ **C:** BrdU positive lens epithelial cell nuclei were counted in control and *Ehd1 CKO* embryos at E12.5, E14.5 and E16.5. *$p < 0.01$. NS, not significant.

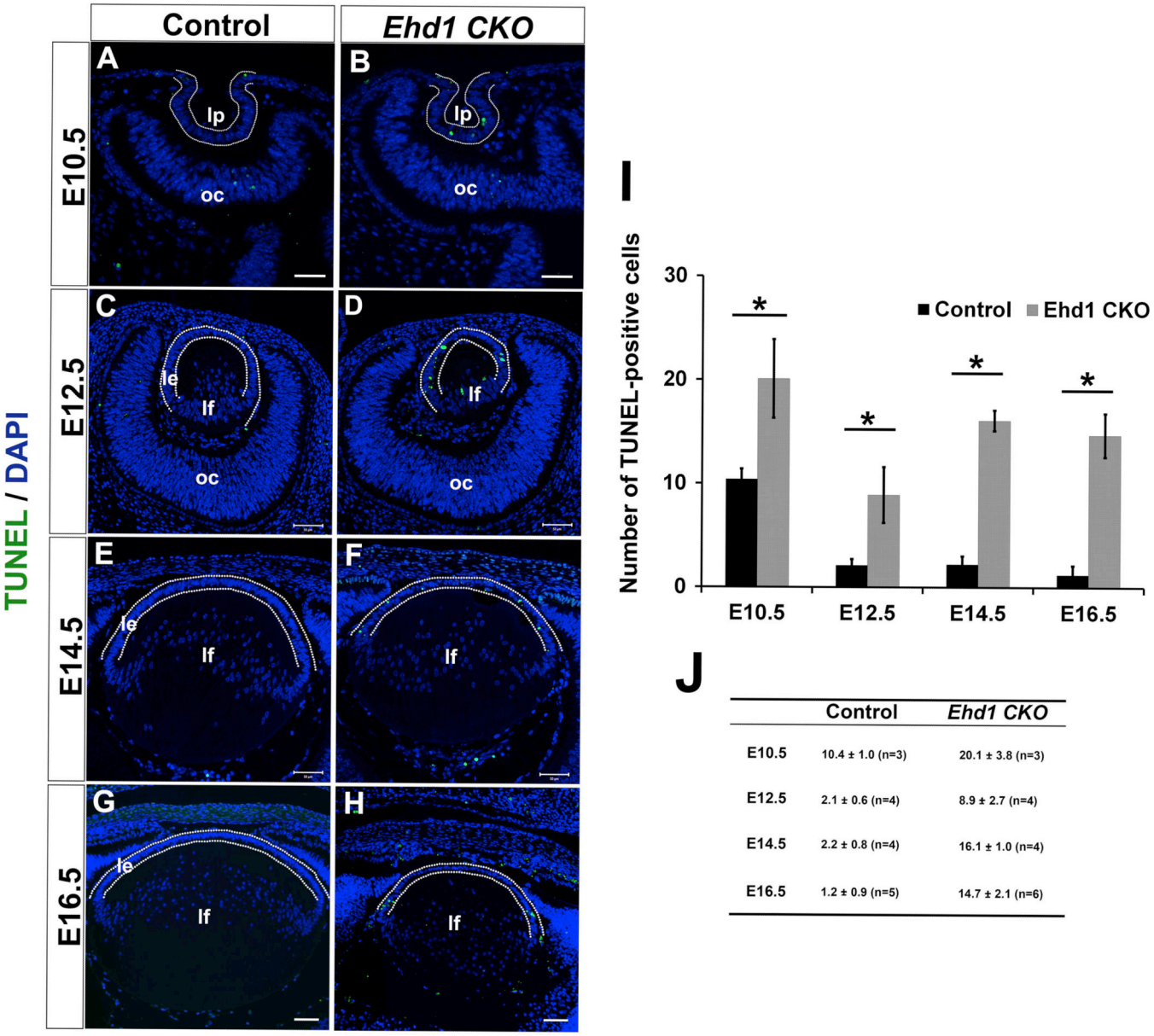

	Control	*Ehd1 CKO*
E10.5	10.4 ± 1.0 (n=3)	20.1 ± 3.8 (n=3)
E12.5	2.1 ± 0.6 (n=4)	8.9 ± 2.7 (n=4)
E14.5	2.2 ± 0.8 (n=4)	16.1 ± 1.0 (n=4)
E16.5	1.2 ± 0.9 (n=5)	14.7 ± 2.1 (n=6)

Fig. 6. EHD1 is required for Cell Survival

A-H: Immunofluorescence staining revealed by TUNEL (terminal deoxynucleotidyl transferase-mediated deoxyuridinetriphosphate nick end-labeling) assay in embryonic sections from control (A, C, E, G) and *Ehd1 CKO* (B, D, F, H) at E10.5 (A, B), E12.5 (C, D), E14.5 (E, F), and E16.5 (G, H). Nuclei are stained blue with DAPI. Increased apoptotic cells (green) are detected in *Ehd1 CKO* mouse lens epithelium. Dotted white lines demarcate the lens region used for the analysis **I-J:** Quantification data from counting of TUNEL-positive nuclei in control and *EHD1 CKO* lenses.*$p < 0.01$; n= number of embryos analyzed. Abbreviations: le, lens epithelium; lf, lens fiber cells; lp, lens pit; oc, optic cup. Scale bar is 50 μm.

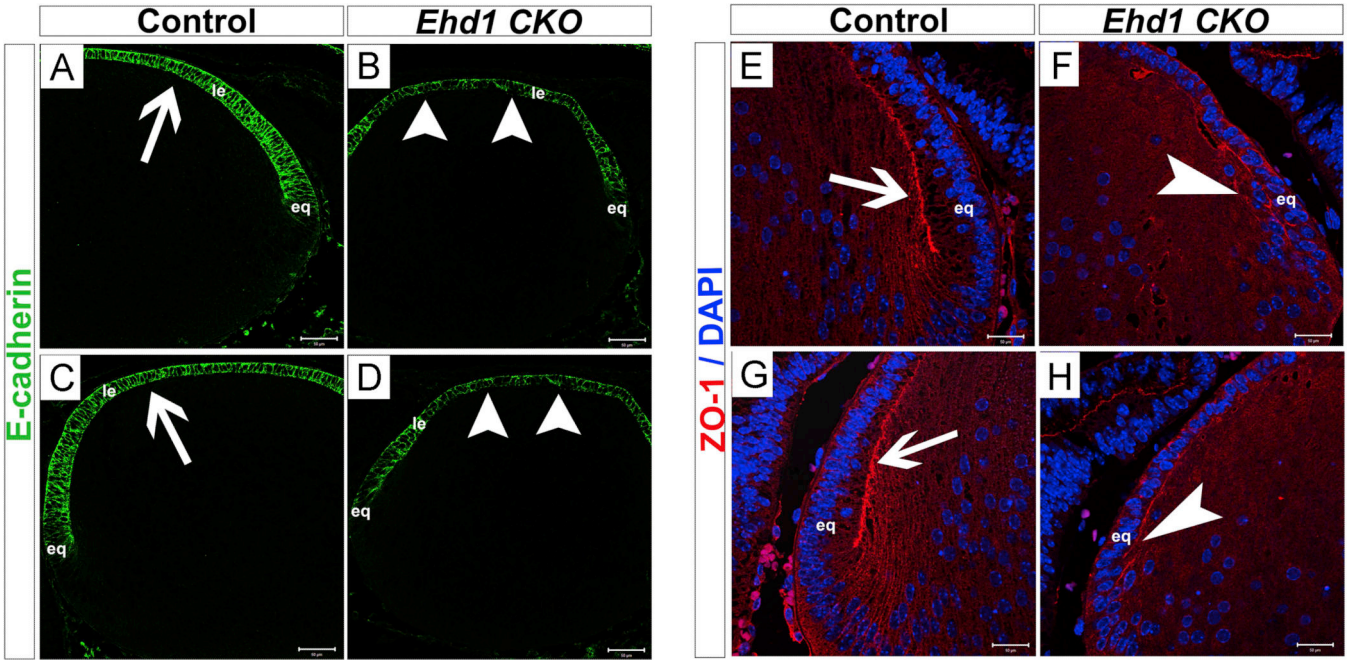

Fig. 7. Altered expression of junctional proteins in *Ehd1 CKO* mice

Formalin fixed paraffin embedded tissue sections from E16.5 are stained for anti-E-cadherin (green) (A–D) and ZO-1 (red) (E–H) antibodies and subjected to confocal fluorescence microscopy. Nuclei are stained blue with DAPI. **A-D:** Normal pattern of expression is evident in control lens (A, C, arrows) whereas in the lens epithelial cells of *Ehd1 CKO*, E-cadherin expression appears disrupted with increased gaps (B, D, arrowheads). **E-H:** ZO-1 expression is irregular and disrupted at the apical lens epithelial junctions in *Ehd1 CKO* mice (F, H, arrowheads) in contrast to the littermate controls (E, G, arrows). At the captured magnification the whole lens structure was not visible within a single frame. Therefore, we included the right side (A, B, E, F) and the left side (C, D, G, H) images to provide a complete representation. Abbreviations: eq, lens equator; le, lens epithelium. Scale bar is 50 μm.

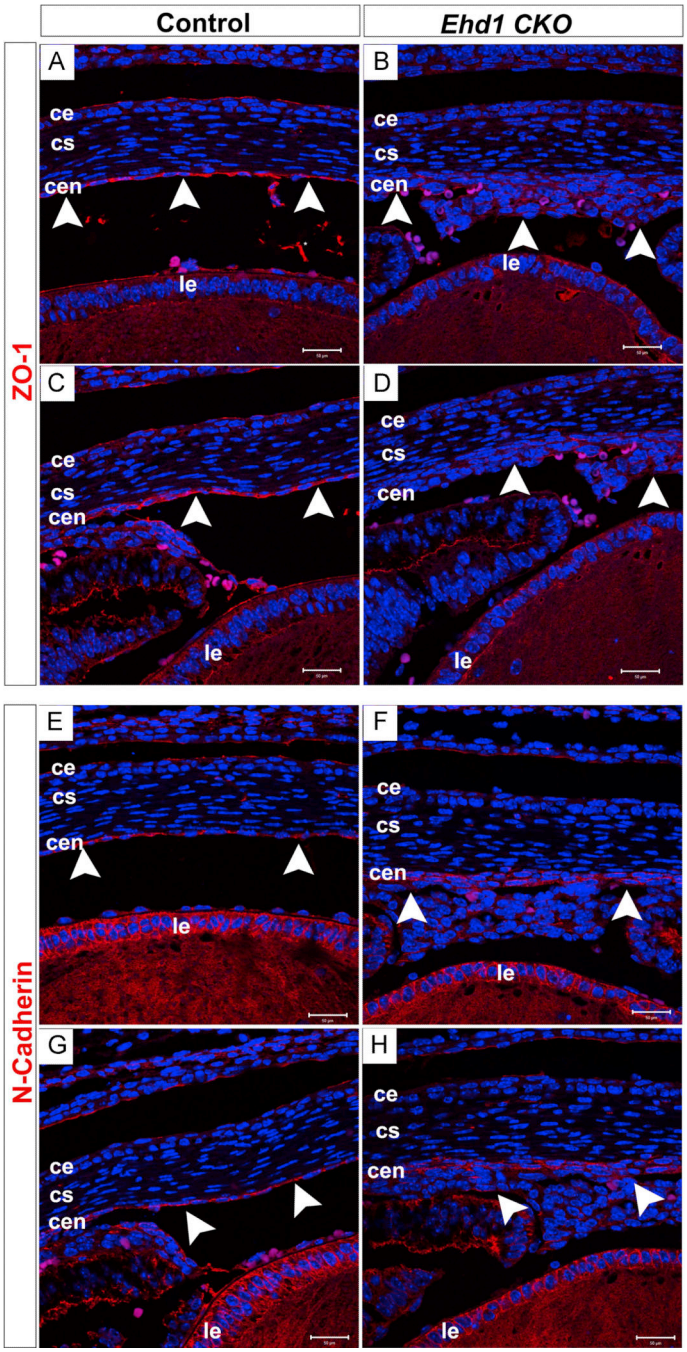

Fig. 8. Corneal endothelium differentiation defects in *Ehd1 CKO* mice

A-D: ZO-1 expression is almost completely lost from the anterior segment and corneal endothelium (B, D arrowheads) of *Ehd1 CKO* eyes, in contrast to the control (A, C arrowheads). **E-H:** In the control eyes, N-cadherin expression is localized to the corneal endothelial layer in the anterior chamber (E, G arrowheads). In the *Ehd1 CKO* eyes, N-cadherin expression was seen in a cluster of cells that accumulate anterior to the lens (F, H

arrowheads). Abbreviations: ce, corneal epithelium; cs, corneal stroma; cen, corneal endothelium; le, lens epithelium. Scale bar is 50 μm.

Table 1

Summary of prevalence of ocular phenotypes in *Ehd1-null* mice. New-born pups were examined at weaning age to determine the range of ocular defects and tabulated under microphthalmia (small eye), anophthalmia (absence of eye) and cataracts (cloudiness of eye). Individual eyes were accounted for tabulation.

	Microphthalmia	Cataracts	Microphthalmia + Cataracts	Anophthalmia	Normal
No. of eyes analyzed (%)	12 (5.7)	55 (26)	11 (5.2)	41 (19.3)	93 (43.8)

Table 2

Summary of prevalence of ocular phenotypes in *Ehd1 CKO* mice. New-born pups were examined at weaning age to determine the range of ocular defects and tabulated under microphthalmia (small eye) and cataracts (cloudiness of eye). Individual eyes were accounted for tabulation.

	Microphthalmia	Cataracts	Microphthalmia + Cataracts	Normal
No. of eyes analyzed (%)	70 (41.7)	39 (23.2)	26 (15.5)	33 (19.6)

Table 3

Summary of prevalence of ocular phenotypes in *Ehd1*$^{flox/+}$. *Le-Cre* mice. New-born pups were examined at weaning age to determine the range of ocular defects and tabulated under microphthalmia (small eye) and cataracts (cloudiness of eye). Individual eyes were accounted for tabulation.

	Microphthalmia	Cataracts	Microphthalmia + Cataracts	Normal
No. of eyes analyzed (%)	70 (41.7)	39 (23.2)	26 (15.5)	33 (19.6)